Physical properties and microstructures in core samples near the Chelungpu fault in Taiwan

Christian DAVID
Laurent LOUIS
Philippe ROBION
Fabien HUMBERT

Teng-fong WONG
Natalie T. CHEN

Anne-Marie BOULLIER

Sheng Rong SONG

Outline of the presentation :

1) The 1999 Chi-Chi earthquake

2) The Taiwan Chelungpu-fault Drilling Project (TCDP)

3) The methodology

4) The results

5) The conclusion

The Chi-Chi earthquake (21 sept. 1999)

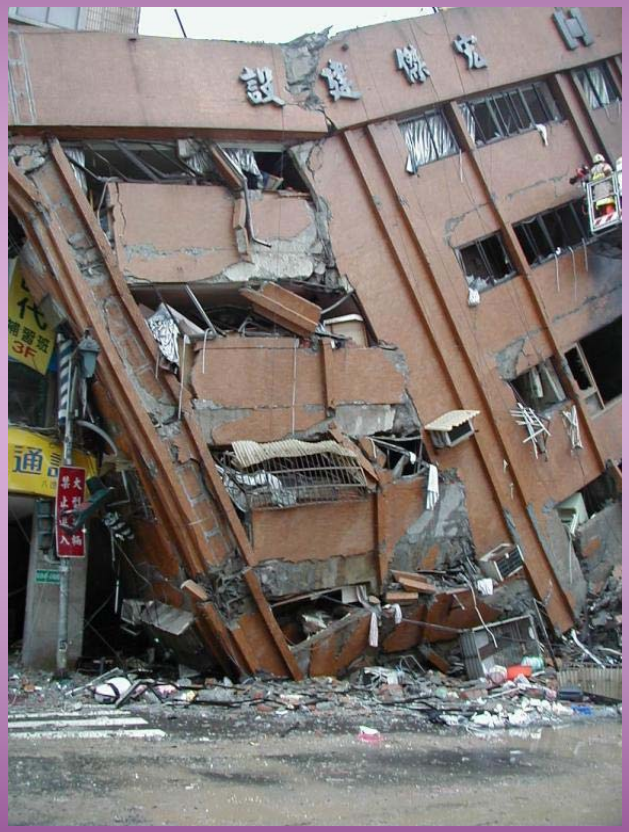

http://www.earth.sinica.edu.tw

Mw : 7.6

Depth :
7 km

Several meters
of uplift

More than 80 000
houses damaged

Associated with
the Chelungpu
thrust fault

The Chi-Chi earthquake (21 sept. 1999)

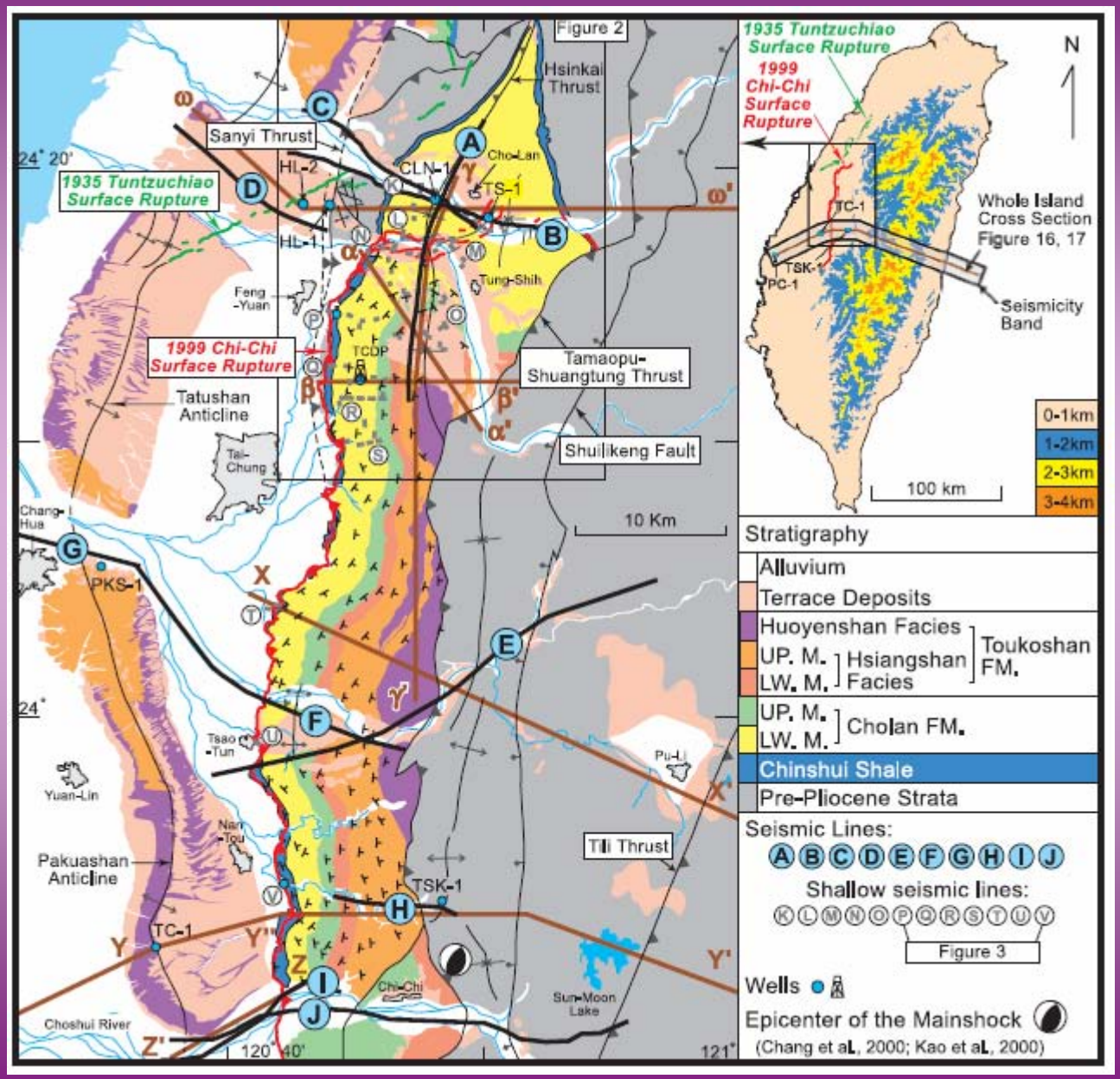

(Yue et al., JSG 2005)

Surface rupture : ~100 km

Seismic slip : up to 10 meters

Larger ground velocity and displacement in the Northern part

Larger acceleration higher frequency in the Southern part

The Taiwan Chelungpu-fault Drilling Project

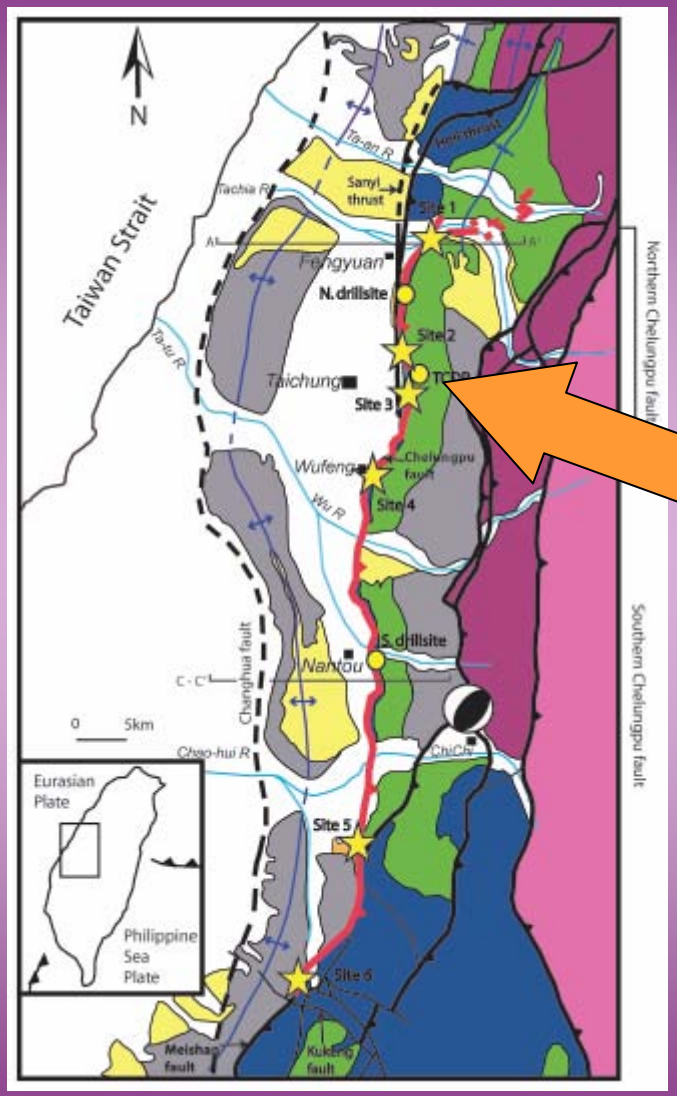

(Isaacs et al., TAO 2007)

TCDP
Taiwan Chelungpu-fault Drilling Project

Initiated in 2002, completed in 2004

International Continental Scientific Drilling Program

icdp

The Taiwan Chelungpu-fault Drilling Project

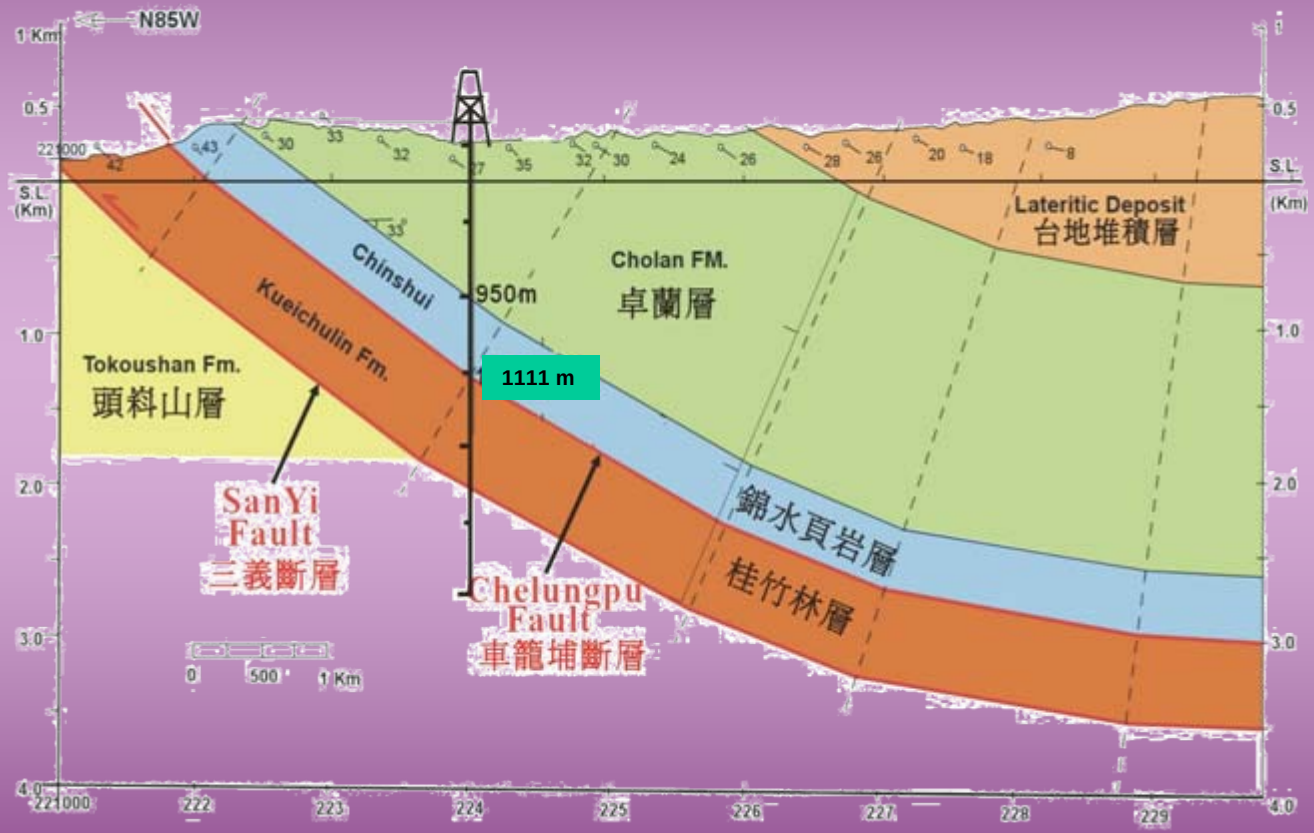

Structural Cross-section for TCDP Drillsite

Two boreholes :

TCDP Hole-A
depth 2003 m
rupture zone
at 1111 m

TCDP Hole-B
40 meters apart
depth 1352 m
rupture zone
at 1136 m

The Taiwan Chelungpu-fault Drilling Project

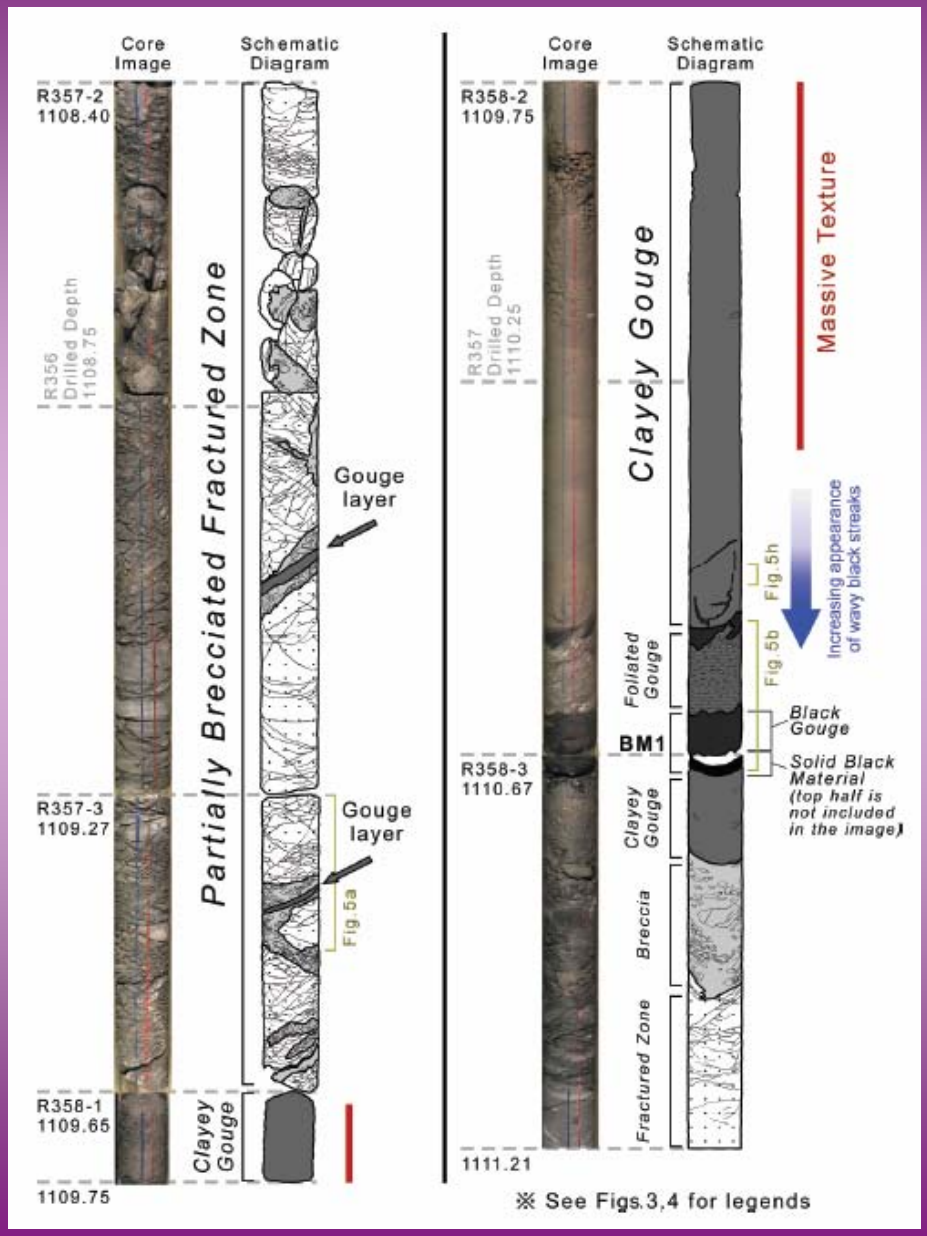

(Sone et al., TAO 2007)

Very good core Recovery (> 95%)

Objectives of our study :

1) analyze the anisotropy of several physical properties

   * *magnetic susceptibility*
   * *P wave velocity*
   * *electrical conductivity*

   for core samples at different depths in TCDP Hole-A

2) derive from these measurements information on the microstructures and the rock deformation in the light of the tectonic environment

3) compare with complementary results obtained recently on samples from TCDP Hole-B

Methodology

Anisotropy of magnetic susceptibility (AMS)

$$\overline{J} = \overline{\overline{K}}\,\overline{H}$$

$$\overline{\overline{K}} = \begin{pmatrix} K_1 & 0 & 0 \\ 0 & K_2 & 0 \\ 0 & 0 & K_3 \end{pmatrix}$$

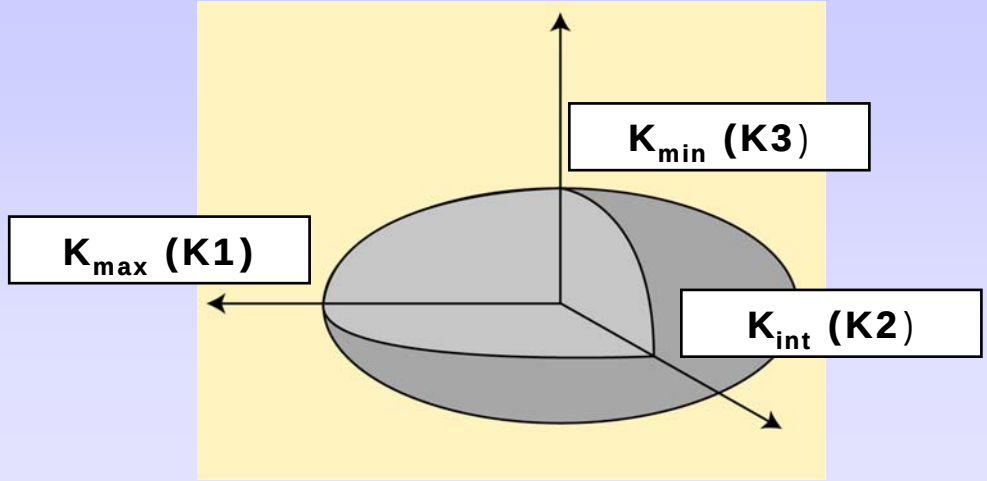

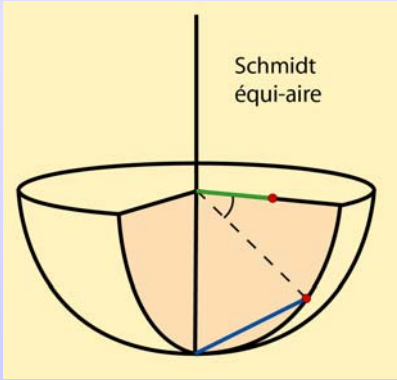

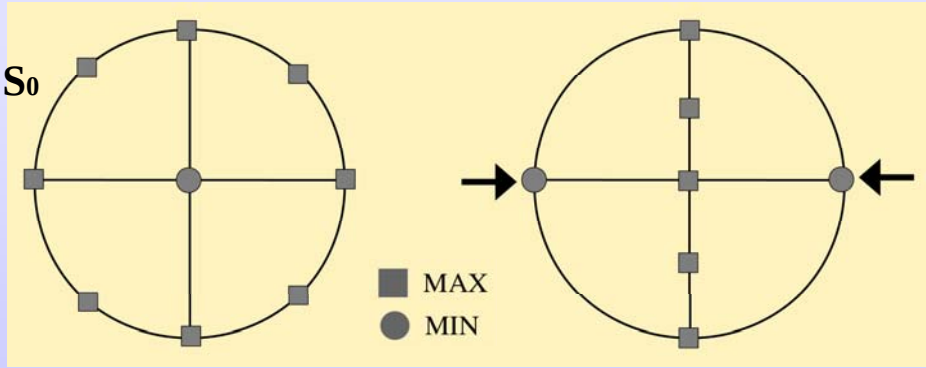

Sedimentary fabric

Tectonic fabric

Methodology

Anisotropy of magnetic susceptibility

Sample size :
diam. 25 mm
length. 22,5 mm

Kappabridge KLY3S (Agico)

Sensitivity of the method :

- cristallographic orientation of phyllosilicates
- orientation and shape of ferromagnetic grains

Methodology

Anisotropy of electrical conductivity (AEC)

Axial measurements on samples cored in 3 orthogonal directions

We don't have access to the full conductivity tensor

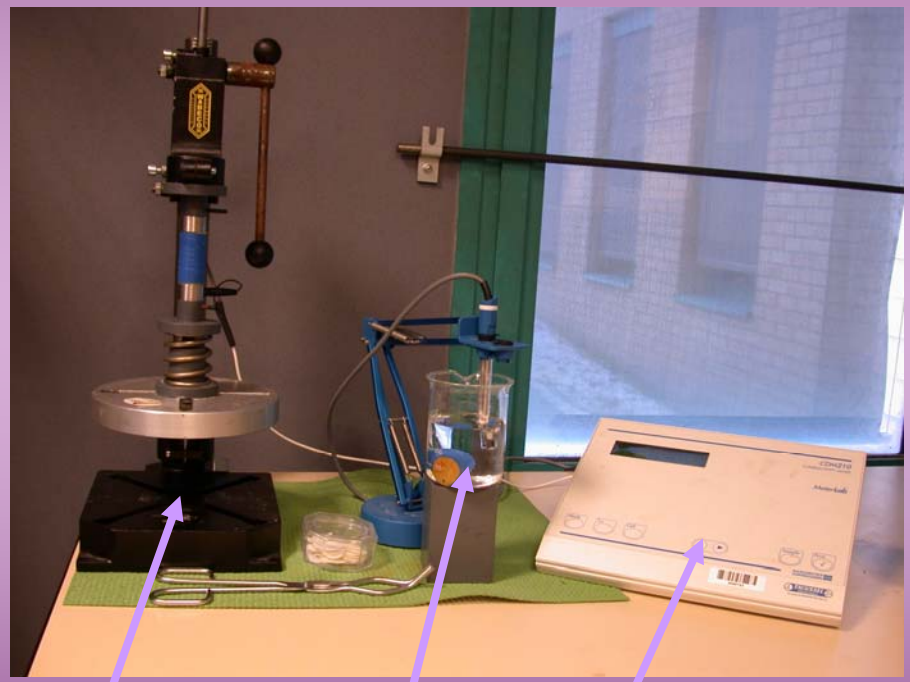

Device for sample conductivity

Cell for measurement of brine conductivity

Conductivimeter

Methodology
Anisotropy of P wave velocity (APV)

Experimental setup for P wave velocity measurements

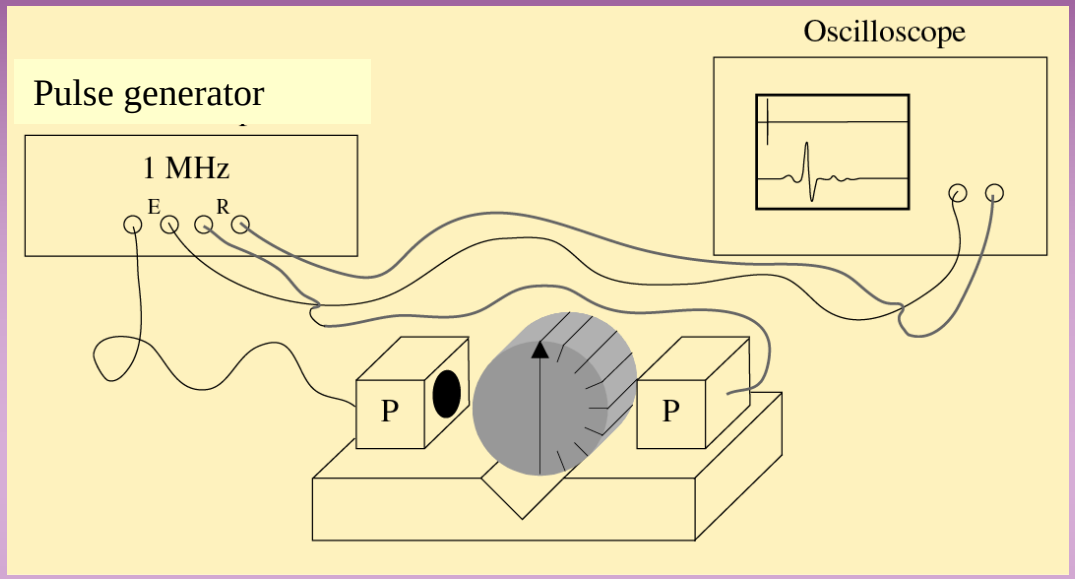

Orientation of samples

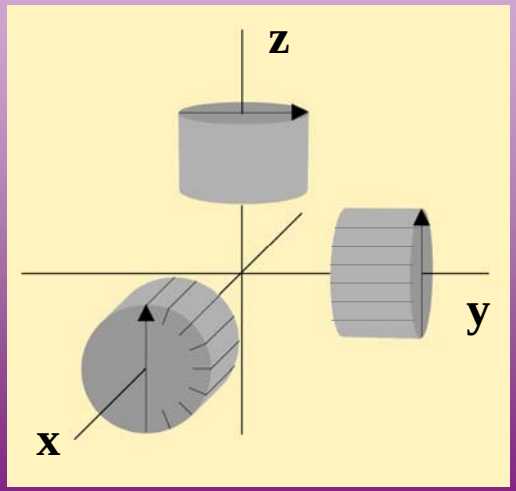

Spatial distribution of measurements

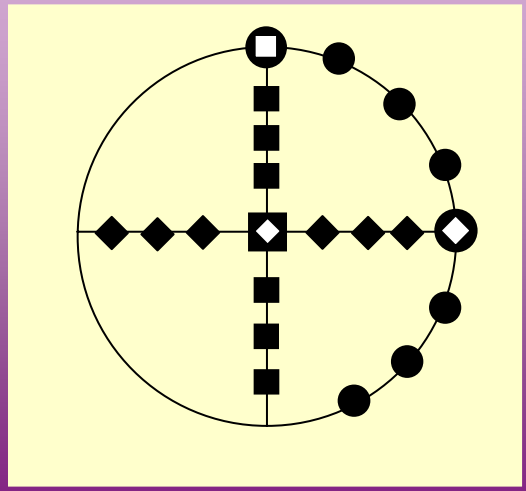

Methodology
Anisotropy of P wave velocity

Louis et al. (2003, 2004)

⇒ determination of a second-rank velocity tensor

Measure

+

Direction

→ **Inversion** → **Representation** → **Interpretation**

$$P = \left({}^{t}Q.Q\right)^{-1}.\left({}^{t}Q.M\right)$$

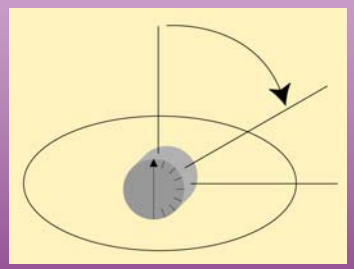

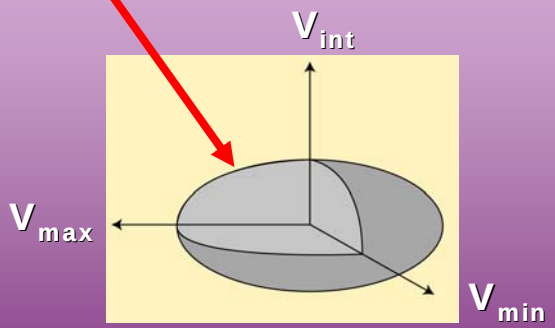

Velocity ellipsoid

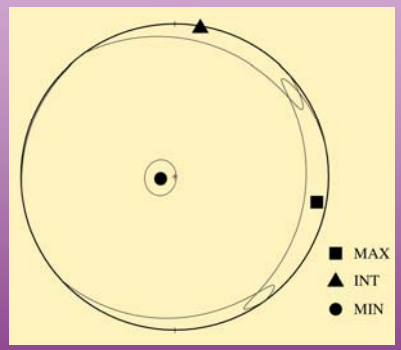

Stereographic plot

relations with observations on :

- **structural data**
- **microstructural data**

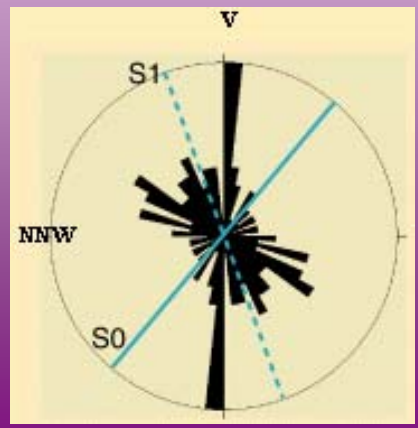

Methodology
Anisotropy of P wave velocity

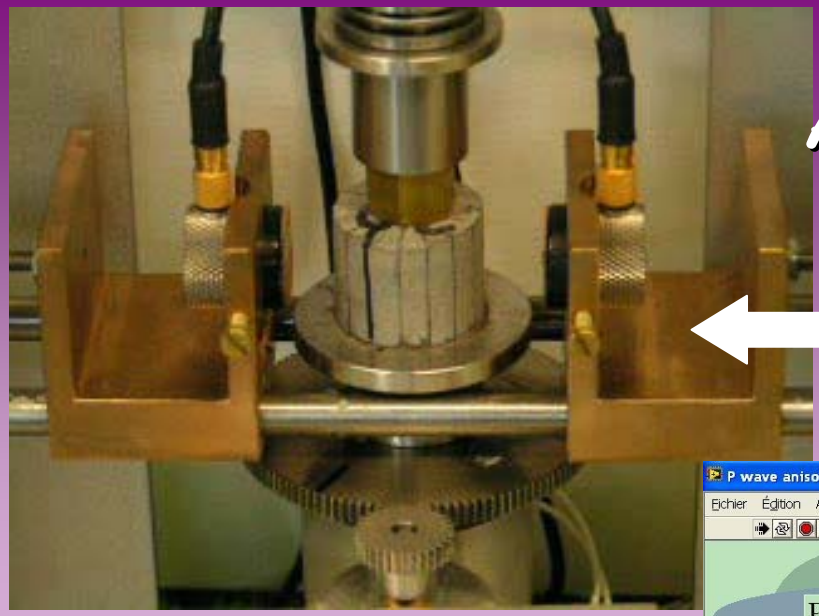

Automated device for directional P wave velocity measurements

duration of one rotation + measurement cycle

10 seconds

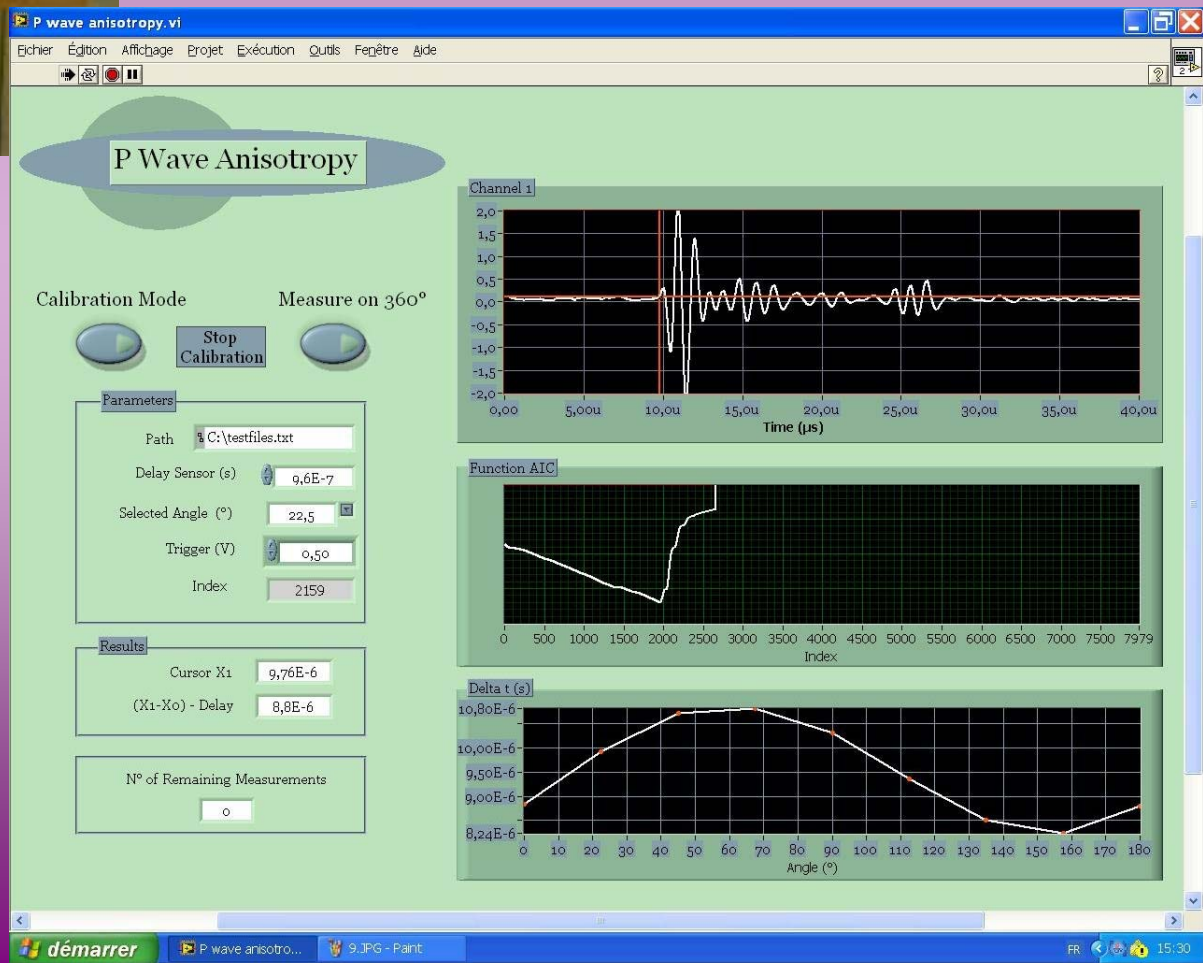

Methodology

Anisotropy of P wave velocity

Sensitivity of the method :
P wave velocity
anisotropy

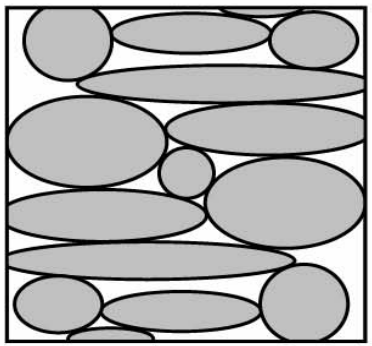

Anisotropy of grains/minerals

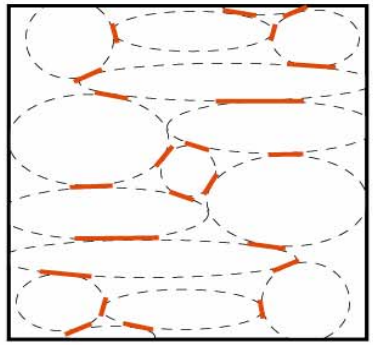

Anisotropy of grains contacts distribution

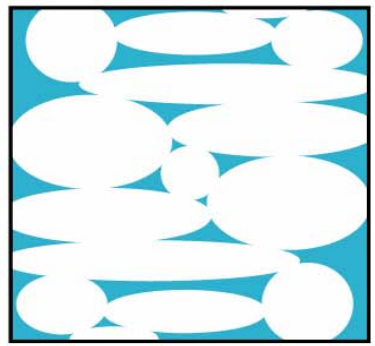

Anisotropy of pore shape

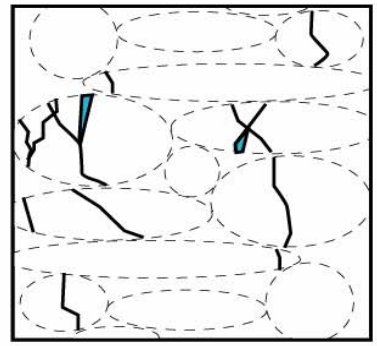

Anisotropy of crack distribution

Example of integrated analysis : COX Shale formation host of the French Underground Research Laboratory for radioactive waste disposal

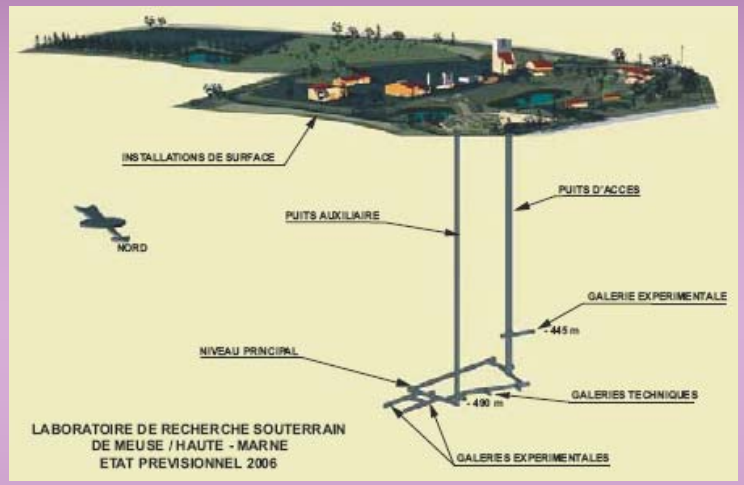

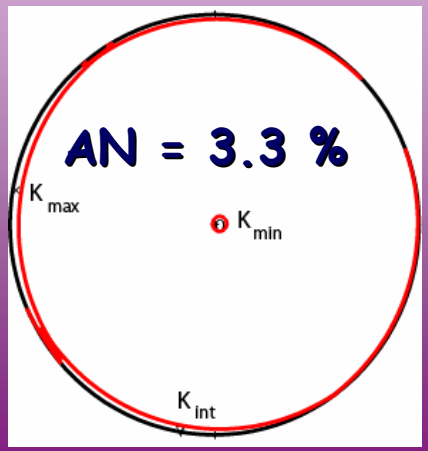

AMS

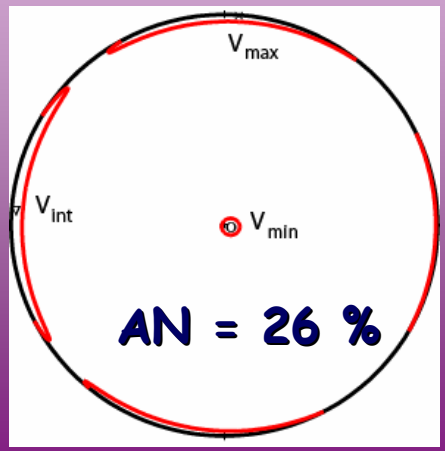

APV

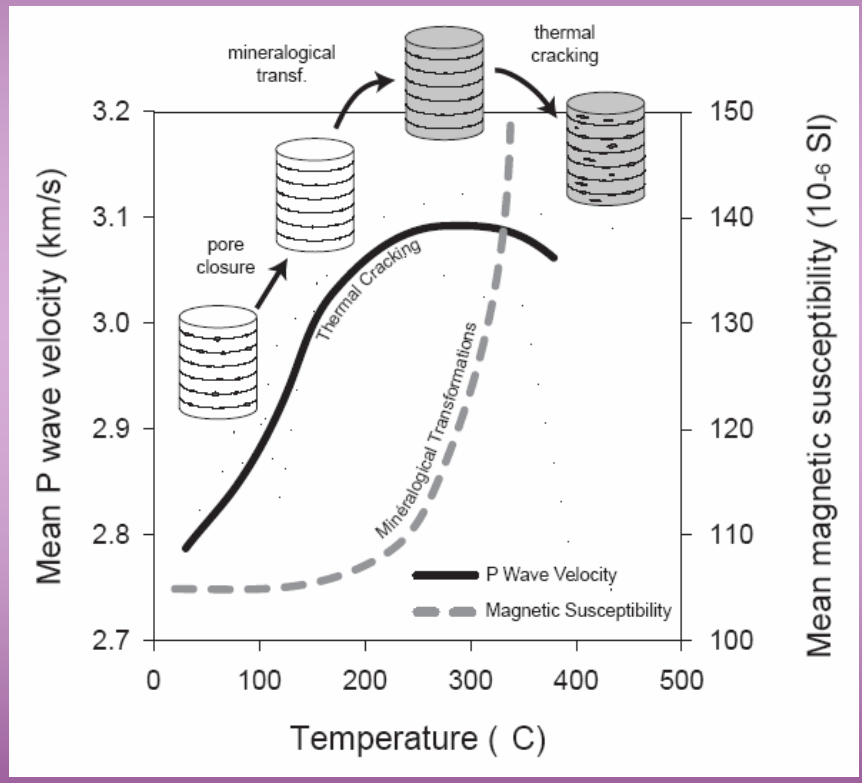

Scenario for the microstructure evolution with temperature

(David et al., PCE 2007; Robion et al., GSL 2007)

Example of integrated analysis : the Chaudrons fold

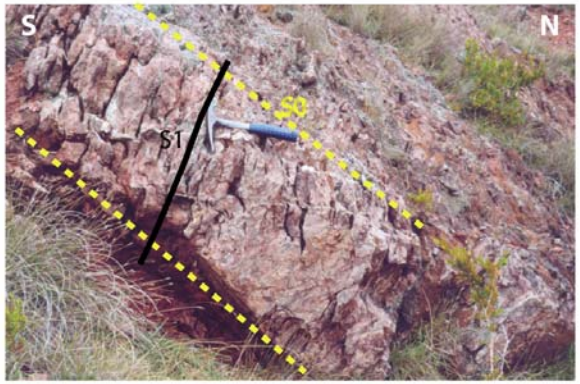

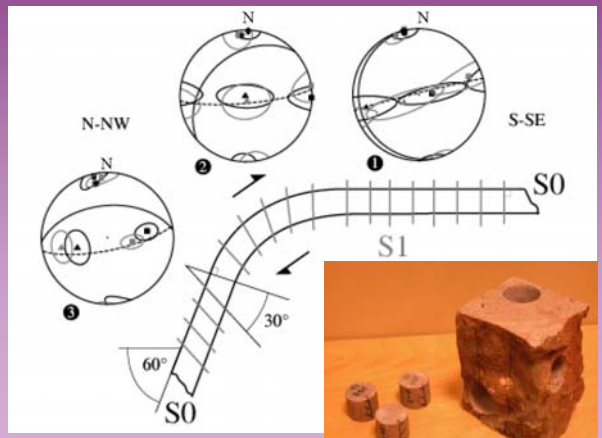

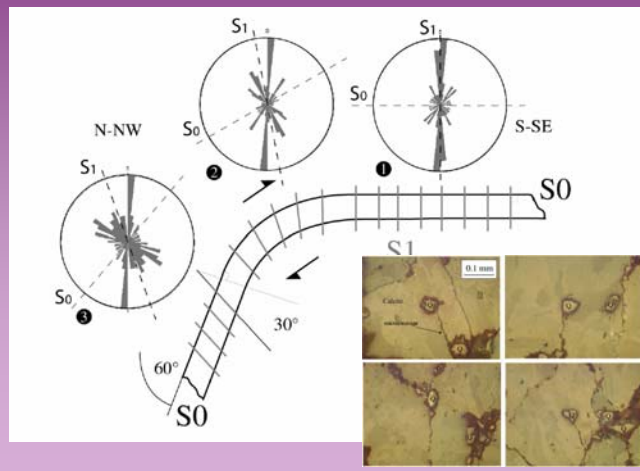

Field scale

Sample scale

Microstructure scale

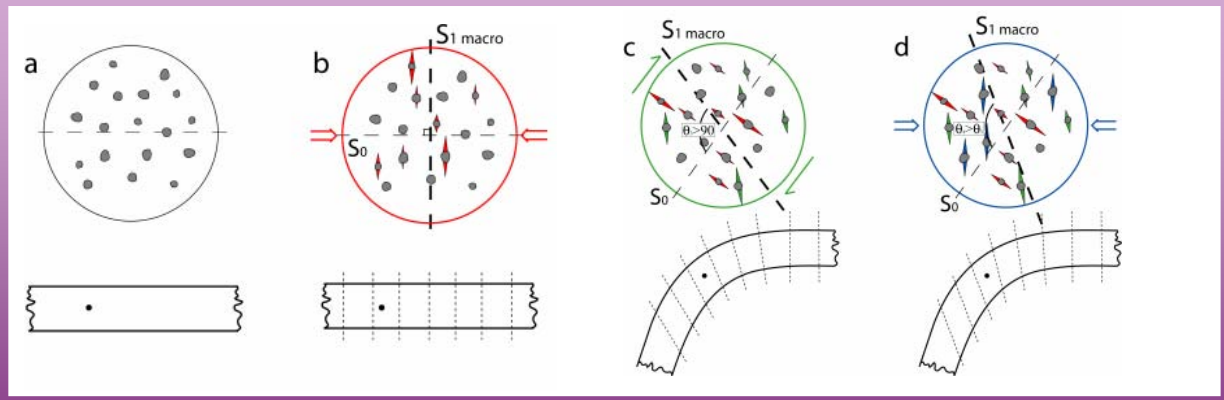

Scenario for the development of microstructures during folding
(Louis et al., JSG 2006)

Results

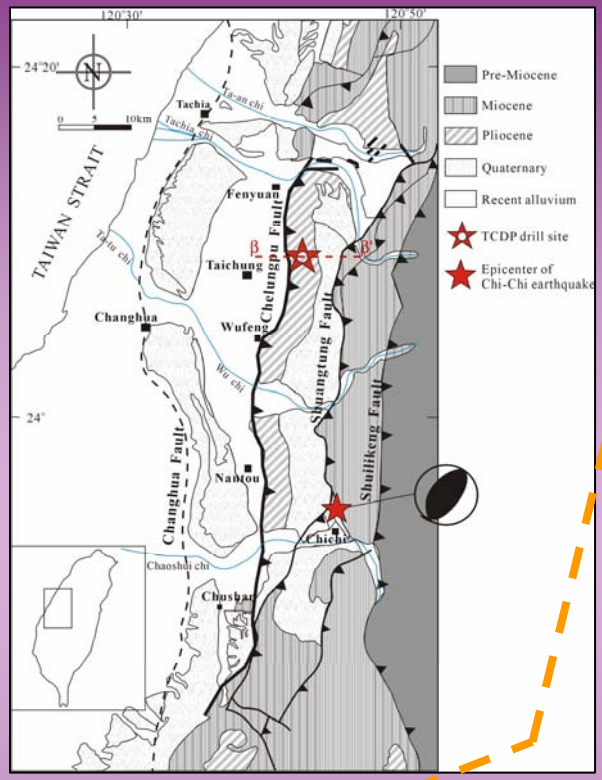

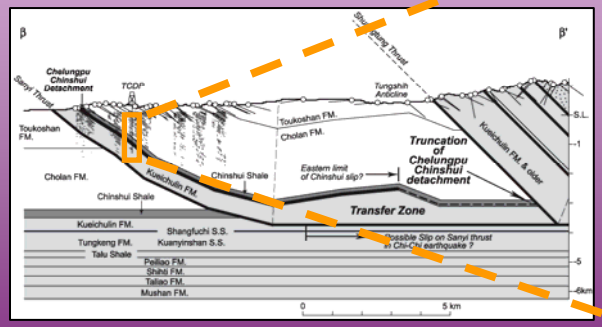

Hole-A

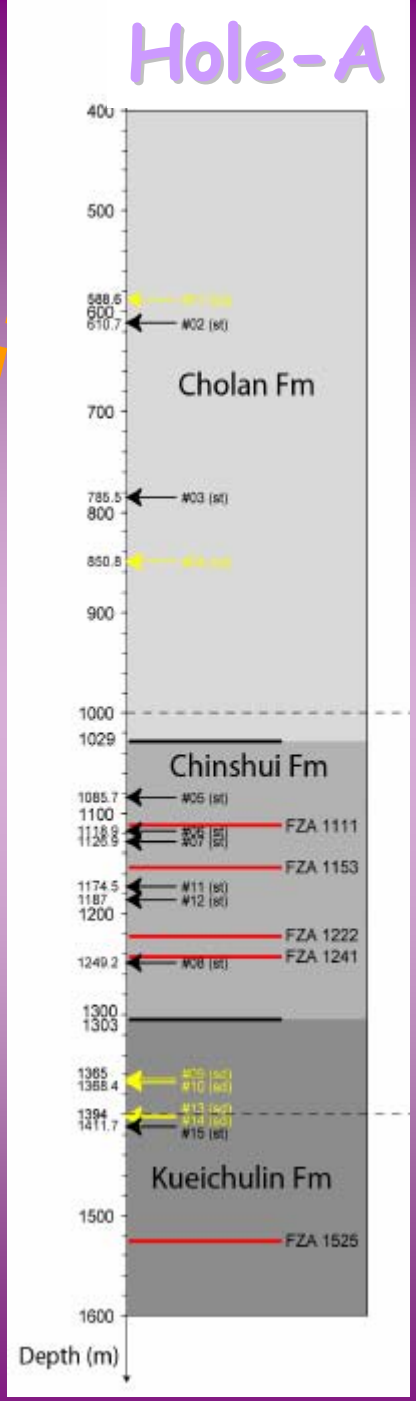

sandstone

siltstone

fault zones

Hole-B

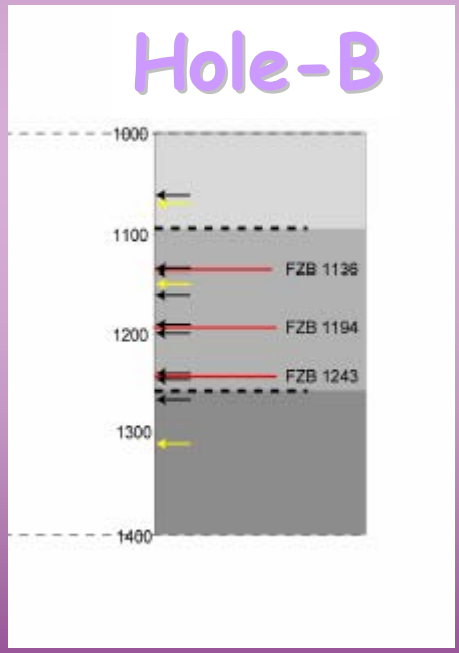

Collection of TCDP Hole-A samples

- Bioturbated sandstone
- No obvious bedding
- Density ~ 2120 kg/m^3
- Porosity: 15-19 %

- Shaly siltstone
- Bedding ~ 30º
- Density ~ 2590 kg/m^3
- Porosity: 4-5 %

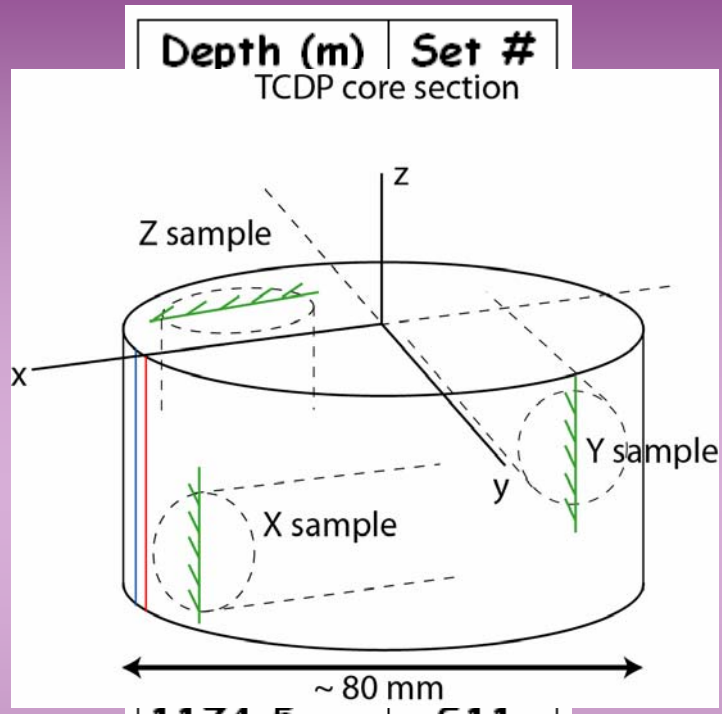

Depth (m)	Set #
1174.5	S11
1187	S12
1394	S13
1394.25	S14
1411.7	S15

Results : AMS

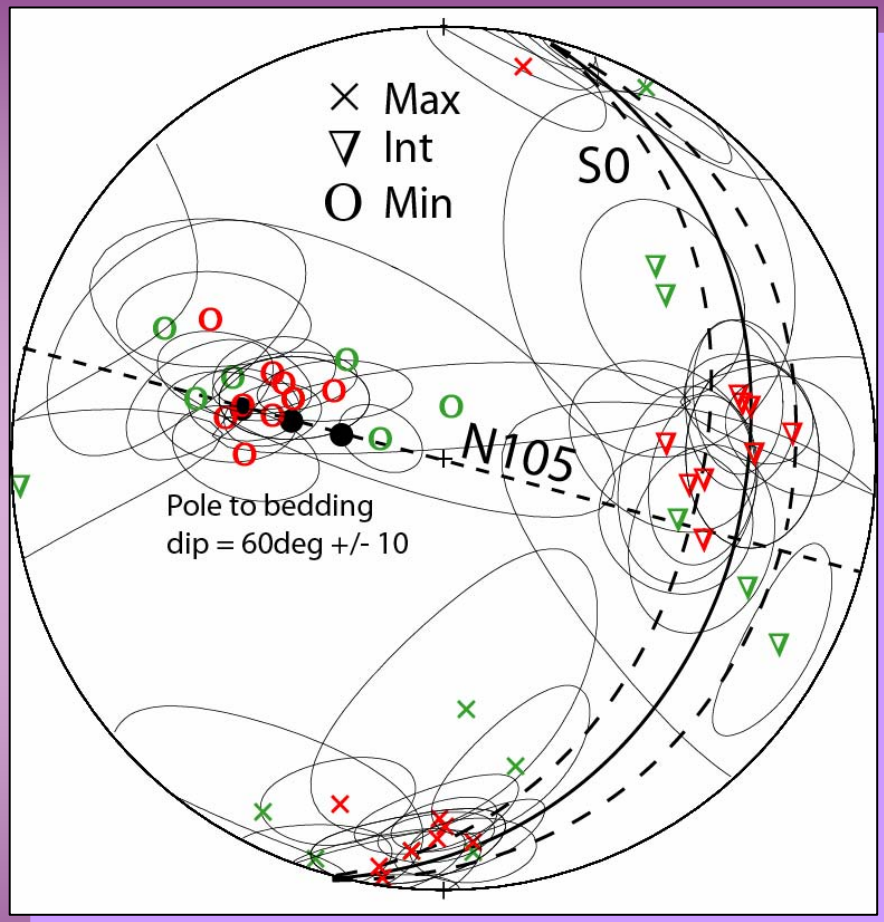

- same orientation for both facies
- triaxial fabric
- minimum axis along bedding pole
- maximum axis along strike

« *layer parallel shortening* »

Red = siltstone
Green = sandstone

Results : APV

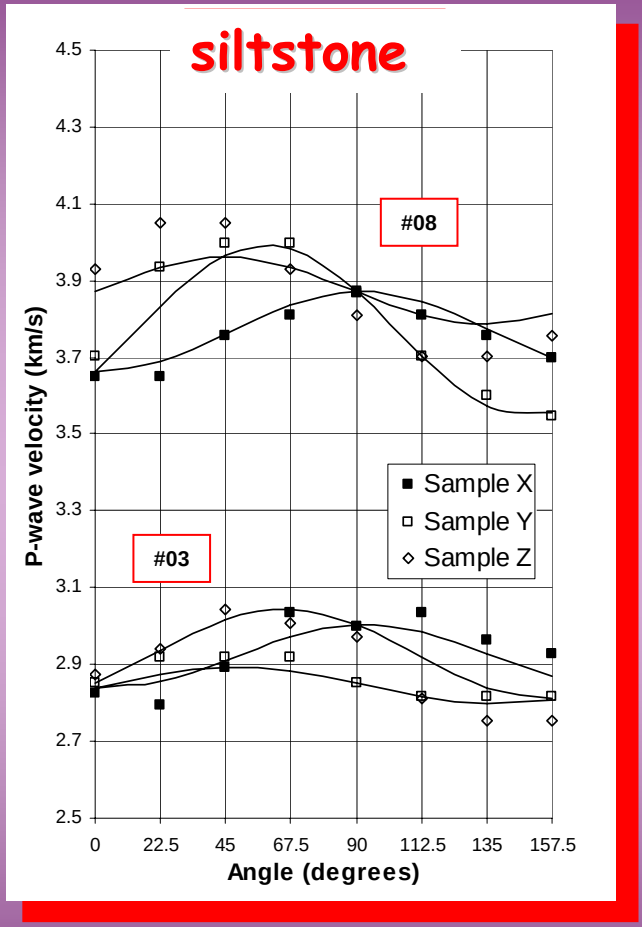

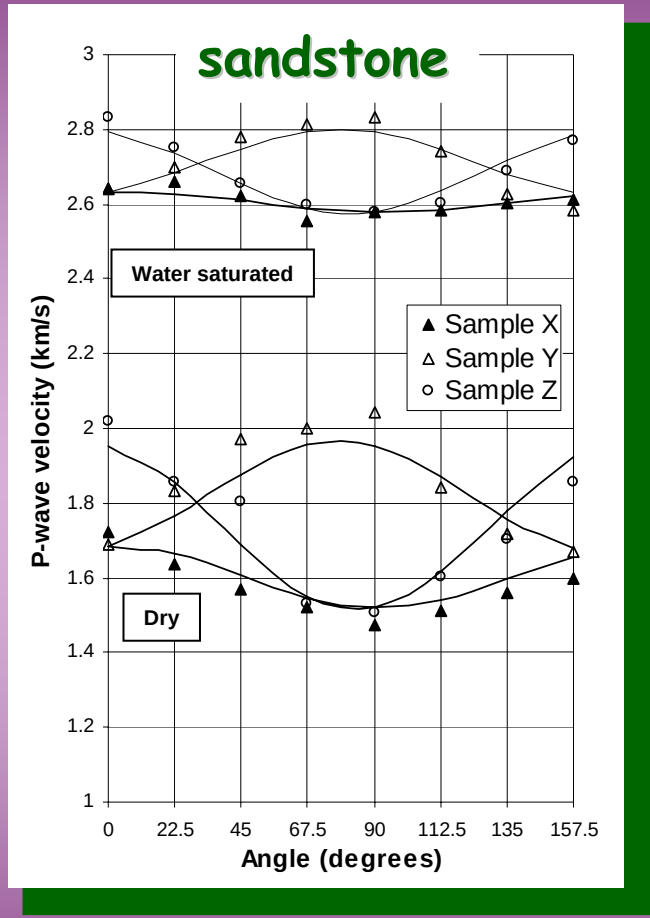

- for siltstones, the P wave velocity depends strongly on density
- for sandstones, measurements on dry and water-saturated samples

Results : APV

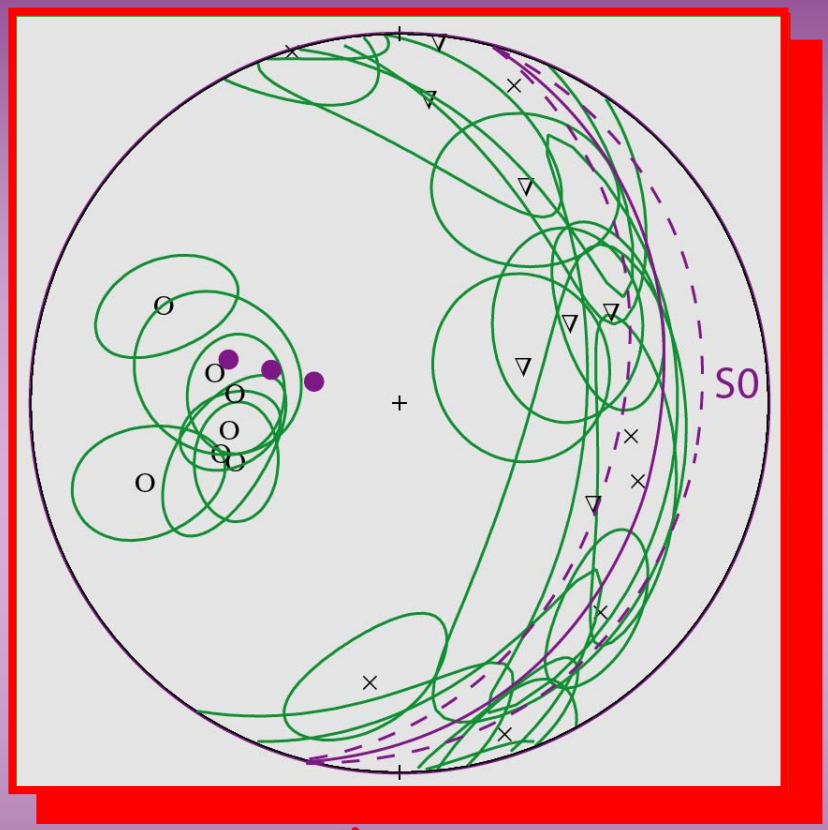

siltstone

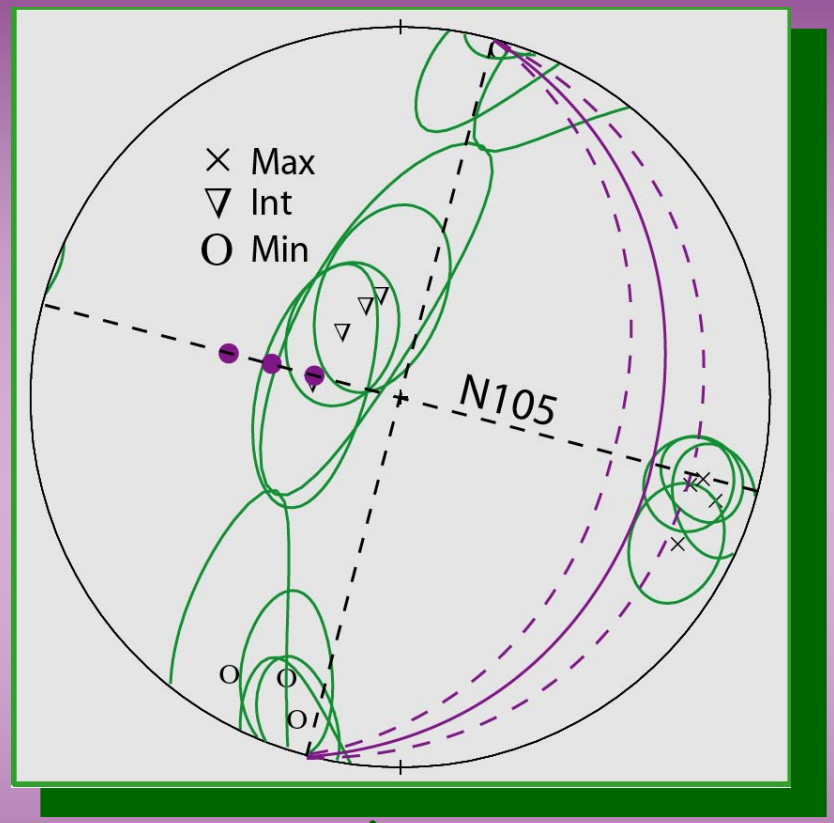

sandstone

- unlike AMS, APV is very sensitive to facies
- for siltstones, similar results as for AMS
- for sandstones, the minimum velocity axis is in the bedding plane, close to the strike

Results : Comparison of AMS and APV

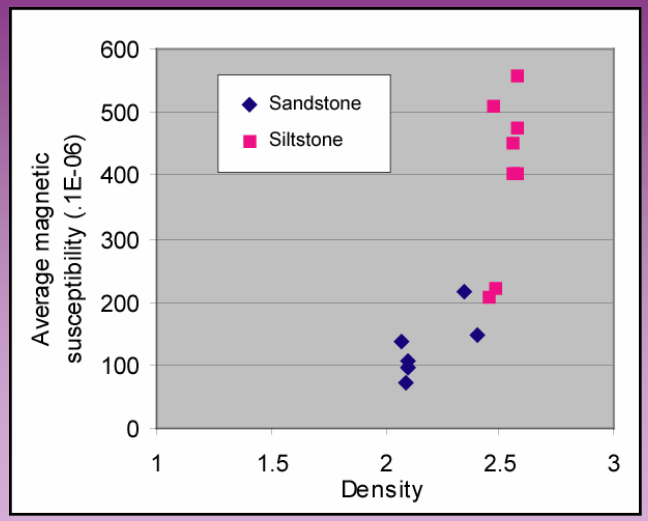

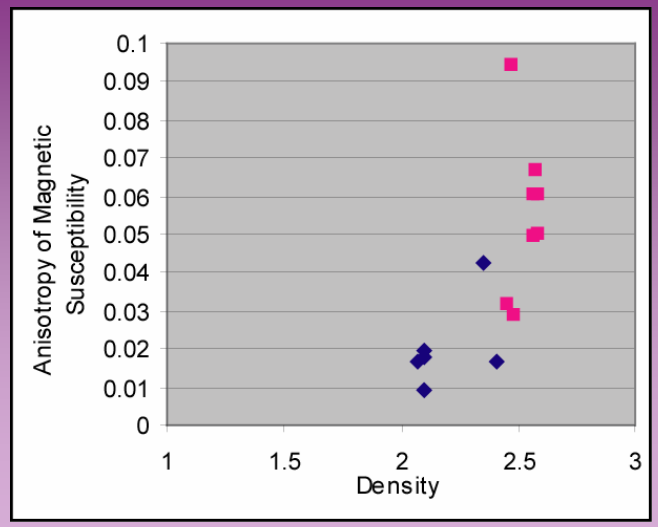

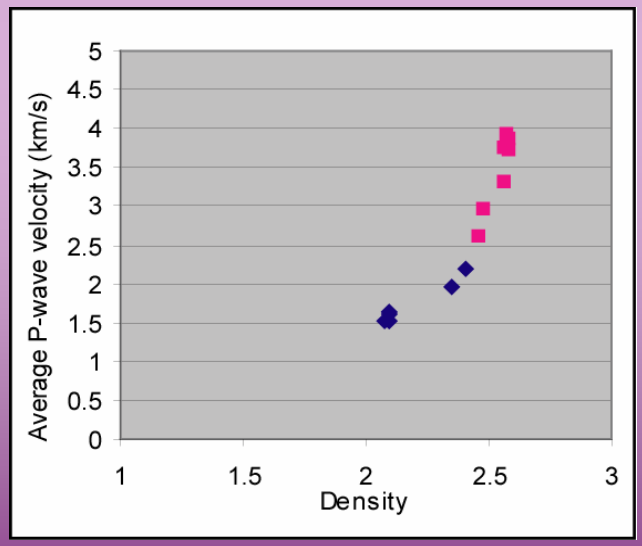

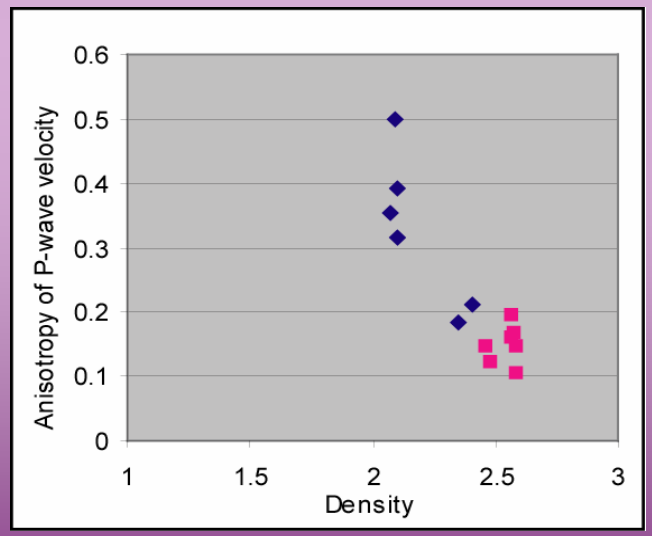

- good correlations with density
- strong P wave velocity anisotropy in sandstones (up to 50% !)
- low magnetic susceptibility anisotropy in sandstones (less than 4%)

Interpretation :

AMS data suggest a weak deformation associated with *layer parallel shortening* in both sandstones and siltstones, at all depths

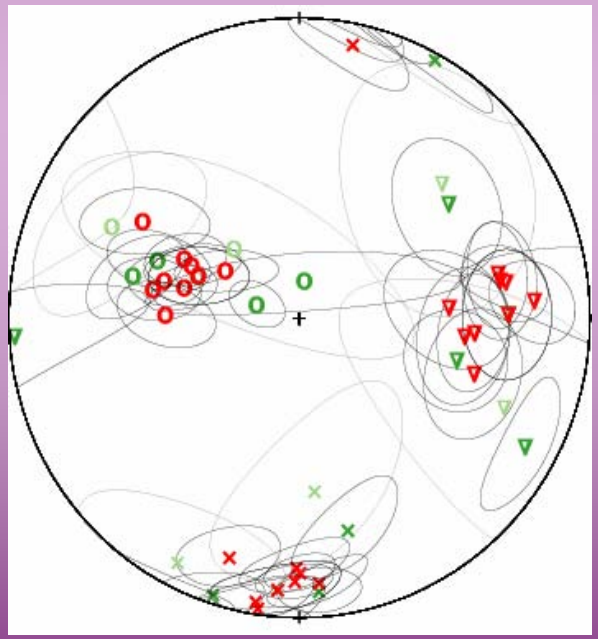

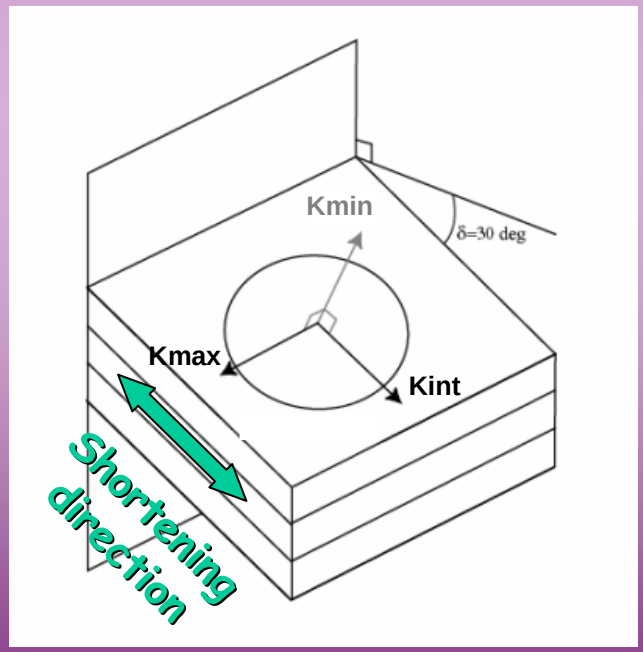

Consistent with elastic fabric only in siltstone

Interpretation :

APV data for sandstones suggest that an additional component of brittle deformation exist which is characterized by an *anisotropic distribution of cracks*

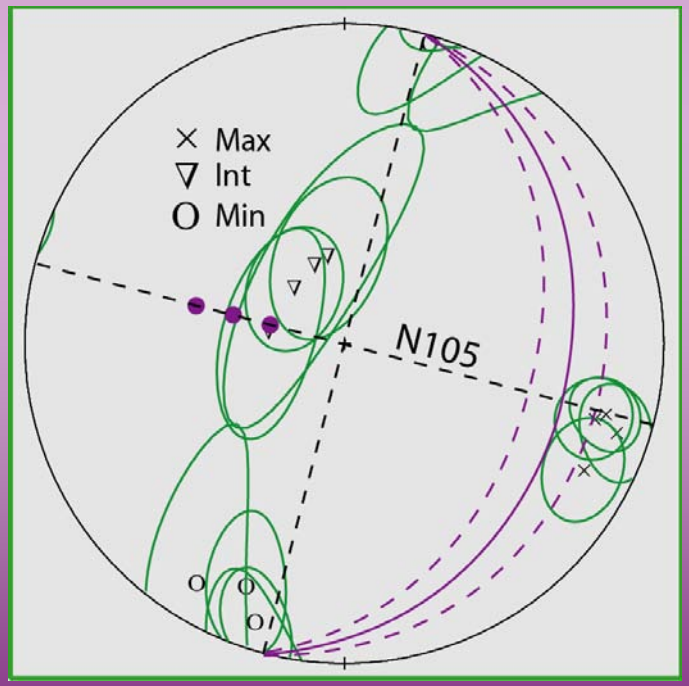

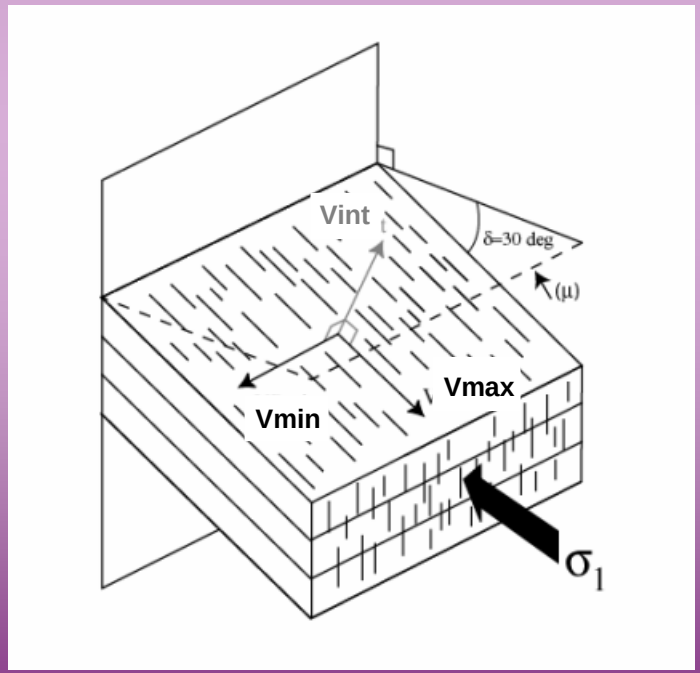

A number of observations support the existence of an anisotropic crack distribution in the sandstone samples

Anisotropy of electrical conductivity

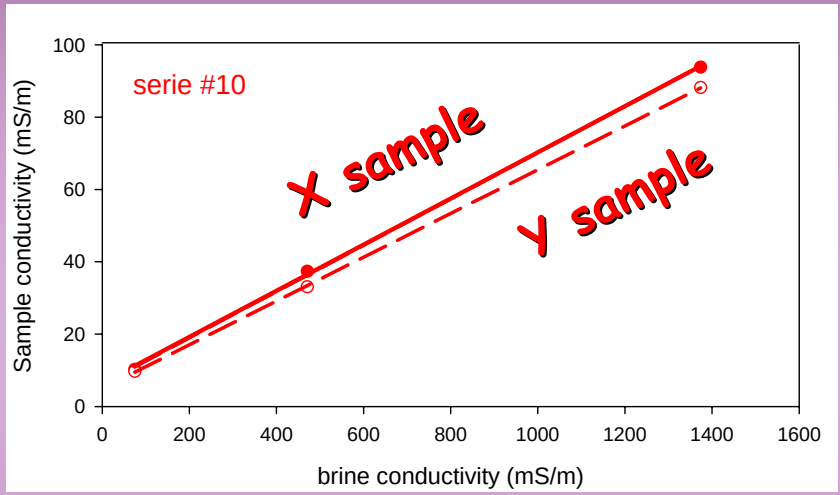

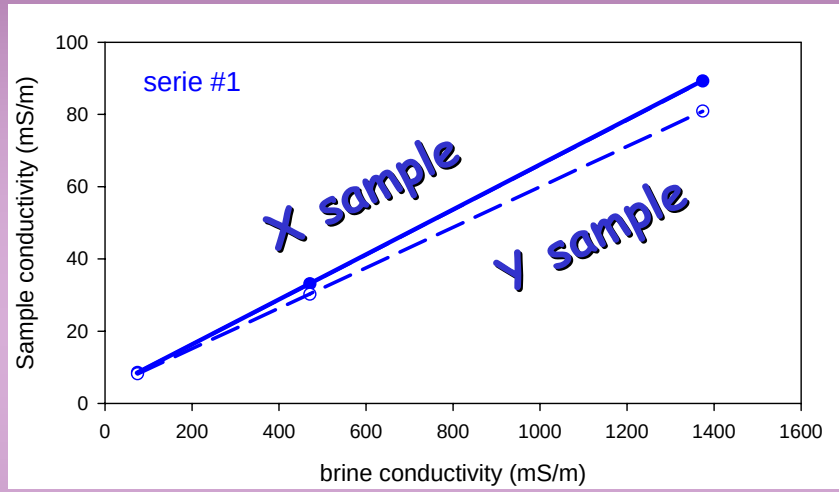

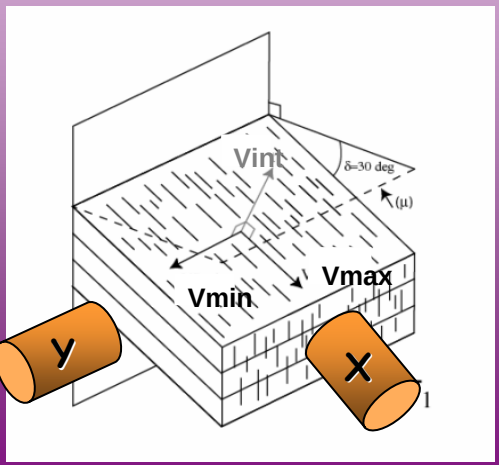

	sample	porosity (%)	Formation factor	surface conductivity (mS/m)	tortuosity
serie #10	X10	19.3	15.6	6.13	3.0
	Y10	19.3	16.5	4.92	3.2
serie #1	X1	18.2	16.1	3.84	2.9
	Y1	18.4	17.8	3.93	3.3

pore fluid effect on acoustic anisotropy

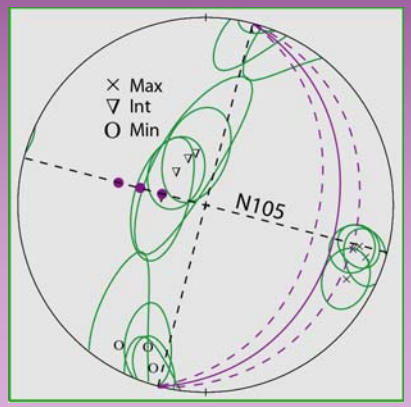

Dry

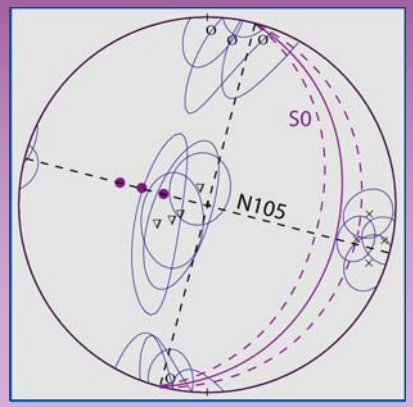

Water saturated

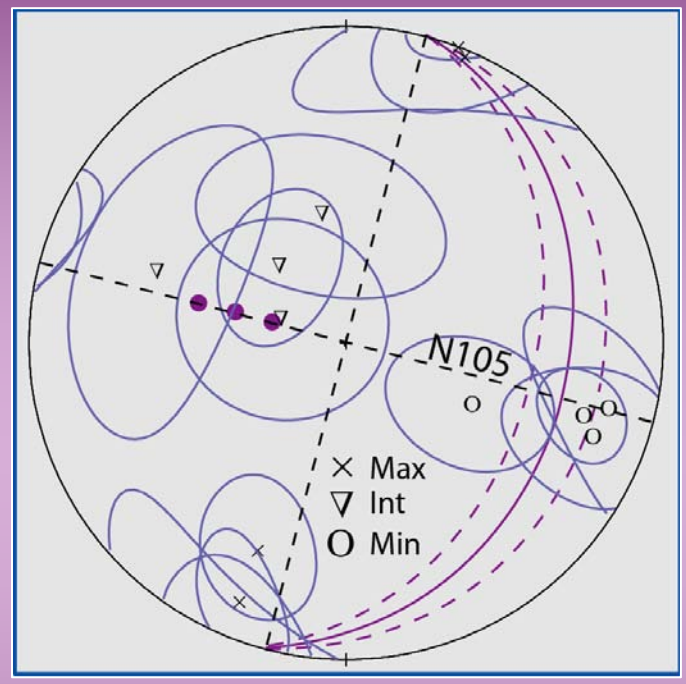

Velocity difference

Depth (m)	set#	Average velocity (km/s)	Anisotropy (%)
Dry samples			
588.6	1	1.53	35.2
1368.4	10	1.53	39.1
Water-saturated samples			
588.6	1	2.59	10.8
1368.4	10	2.43	9.3

Increase of stiffness due to pore-filling is maximum in the direction where the cracks are more compliant

pore shape analysis using AMS on ferrofluid impregnated samples

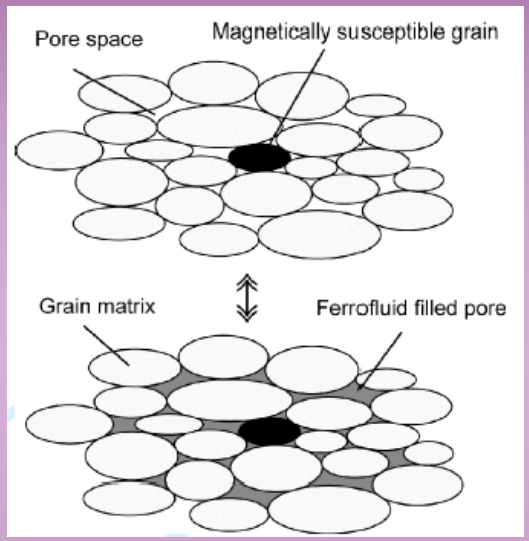

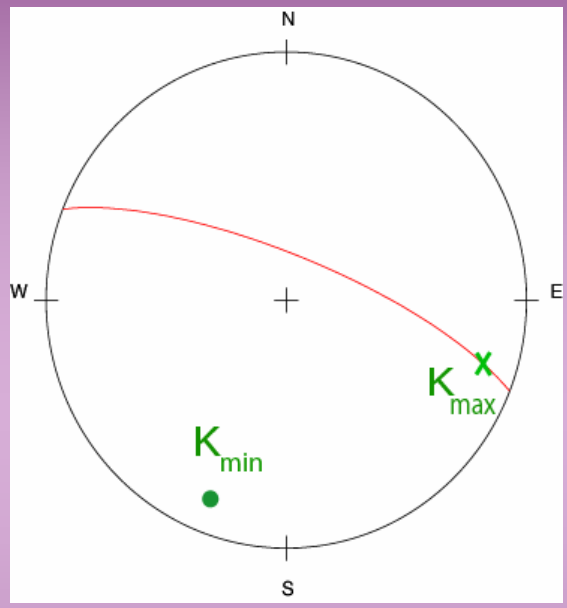

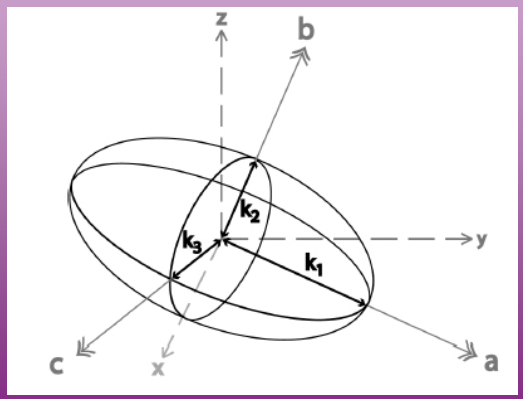

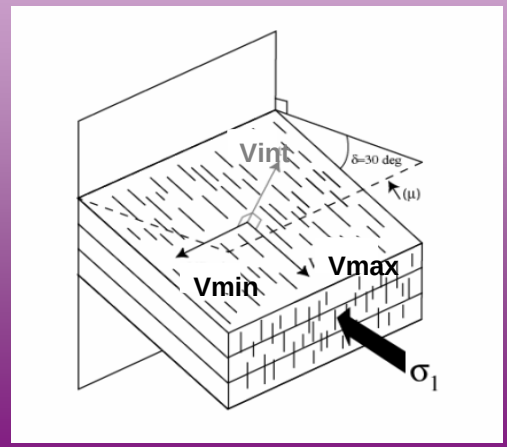

Minimum susceptibility is found perpendicular to the cracks

Maximum susceptibility is found parallel to the cracks

analysis of microstructures

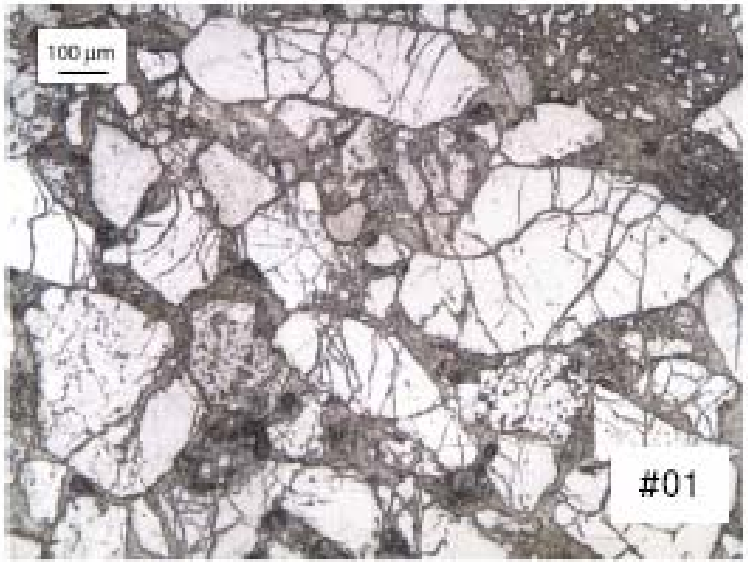

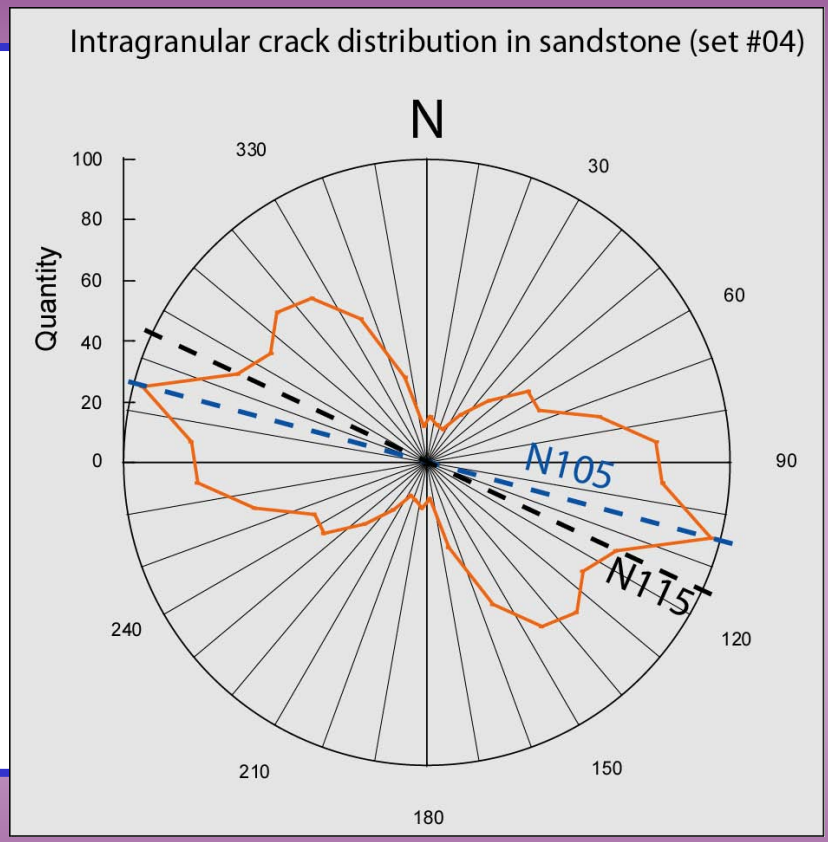

- orientation analysis of about 900 cracks using image analysis tool
- the largest count corresponds to the North 105° in agreement with our analysis on the elastic fabric

analysis of microstructures

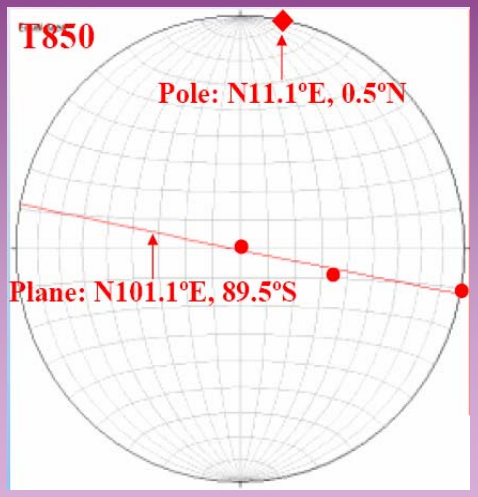

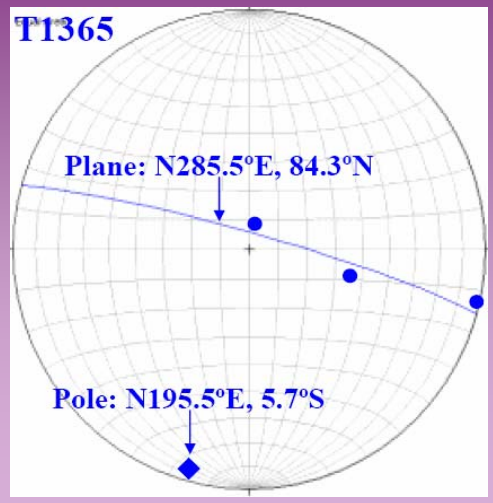

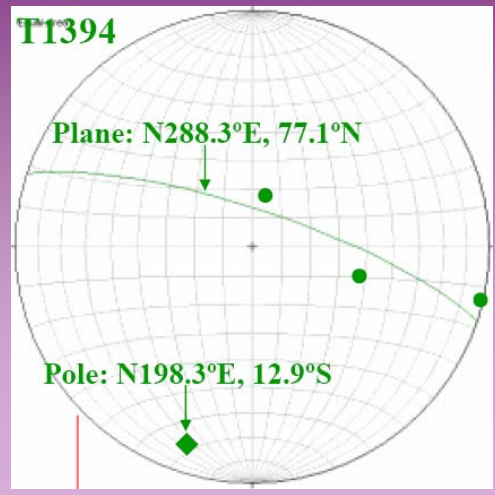

Analysis on 3 orthogonal thin-sections, on sandstone samples at different depths

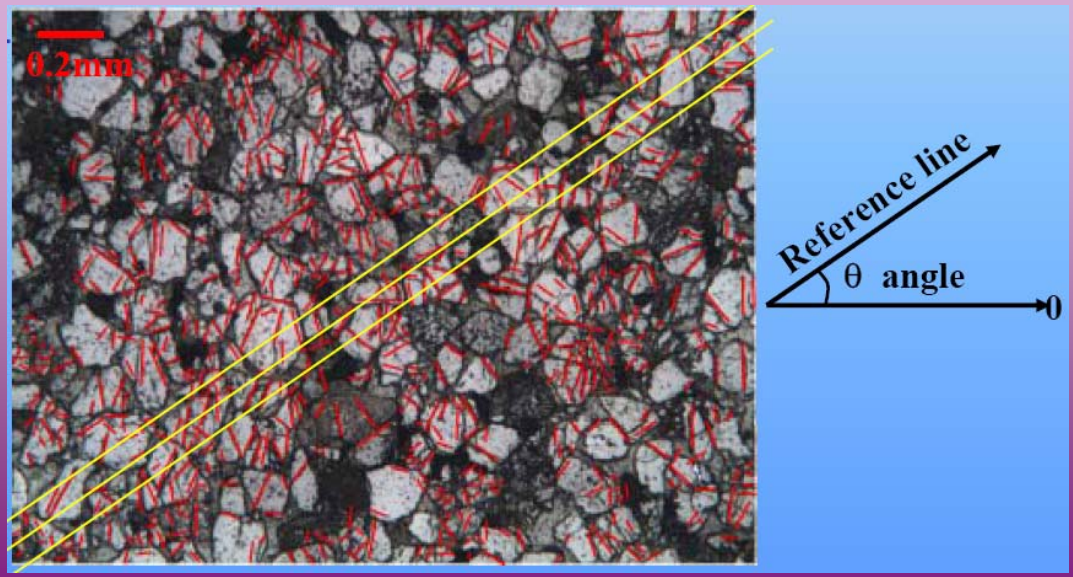

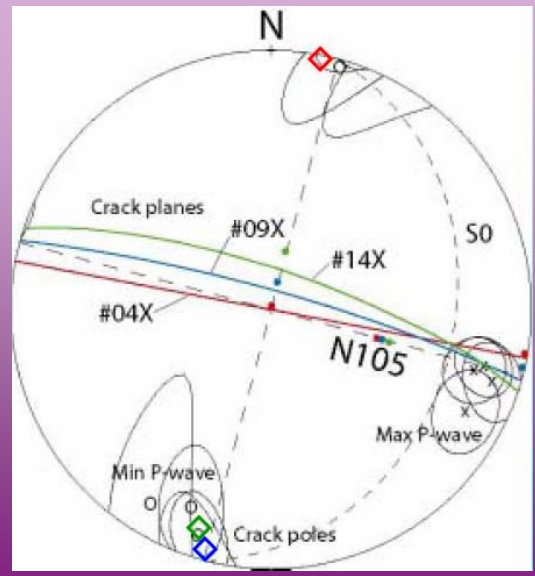

Comparison with tectonic and structural settings

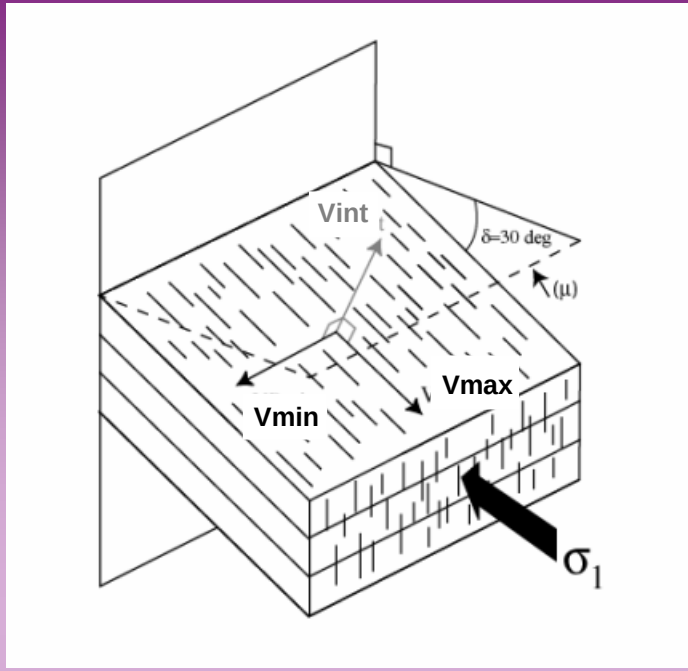

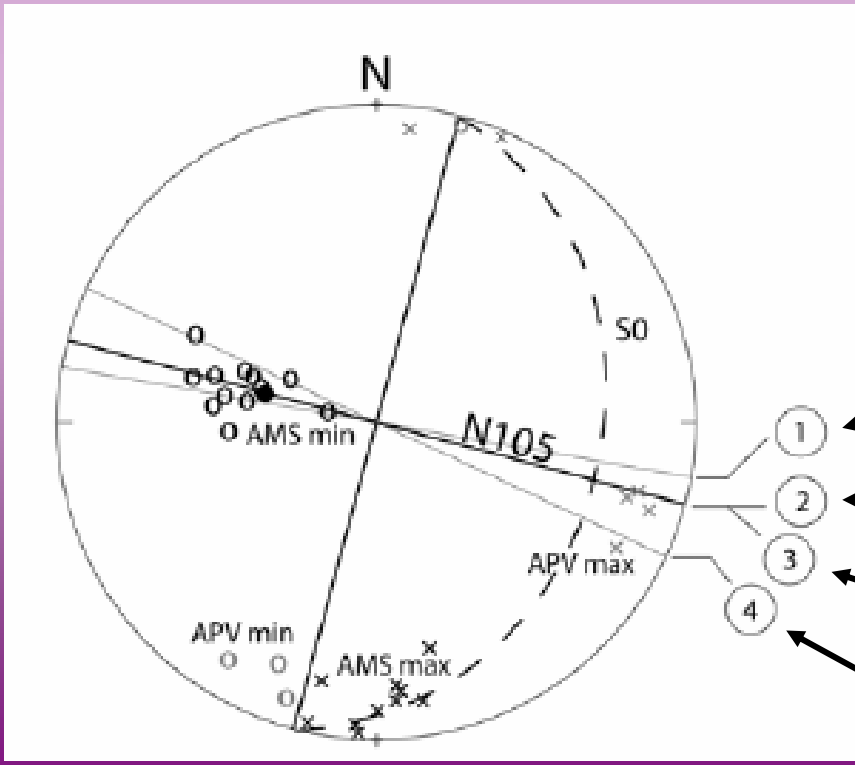

Stress trajectory from fold axes

Paleostress trajectory from fault analysis

Average bedding dip direction in Hole A

S_{Hmax} deduced from borehole breakouts

Recent measurements on spherical TCDP samples under pressure

Petr Spacek
Institute of Earth Physics,
Masaryk University,Czech Republic

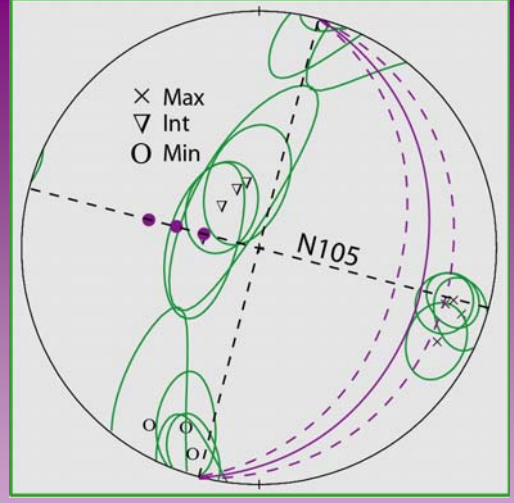

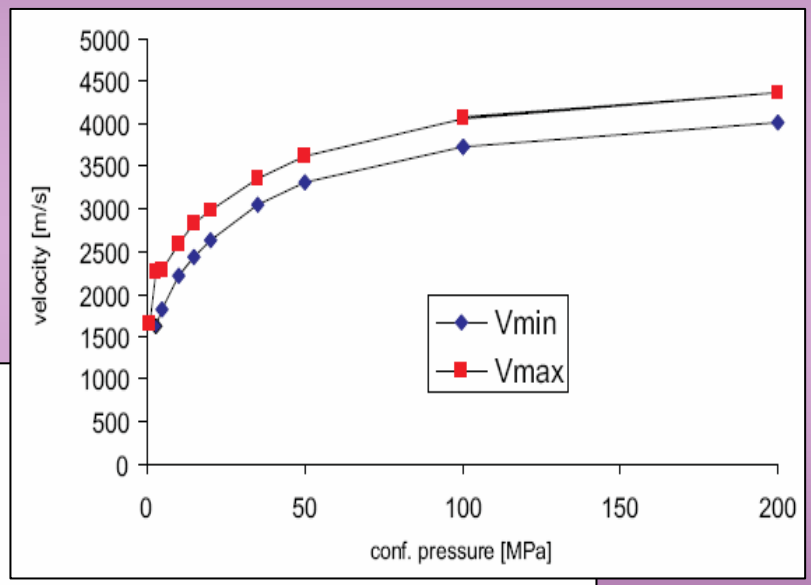

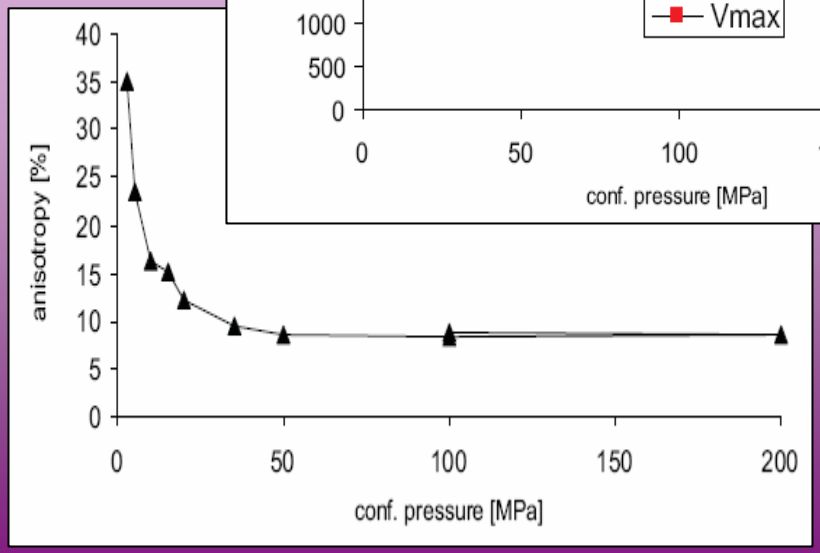

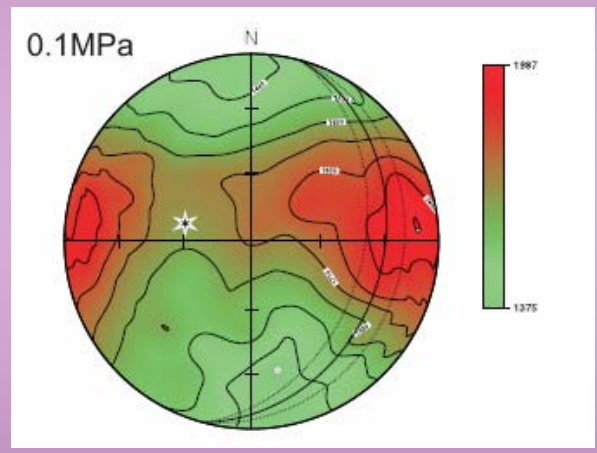

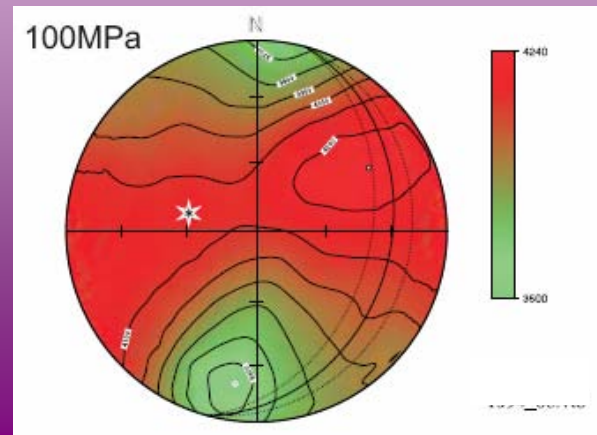

....however there is some problem

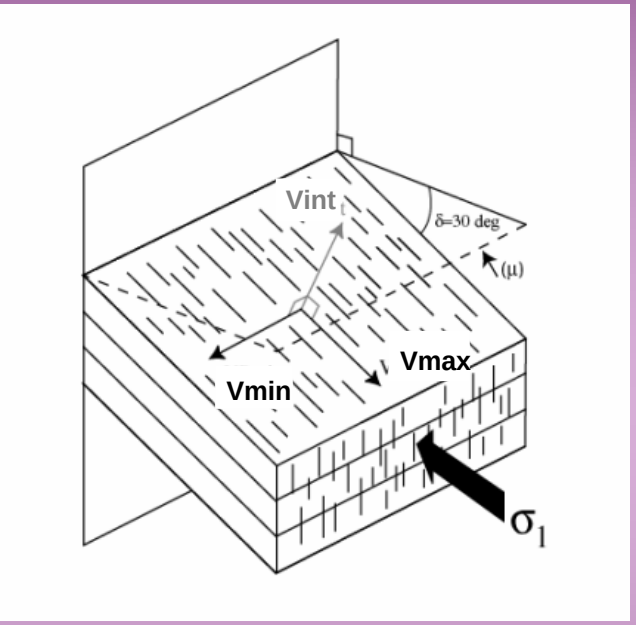

not fully compatible with the present stress field

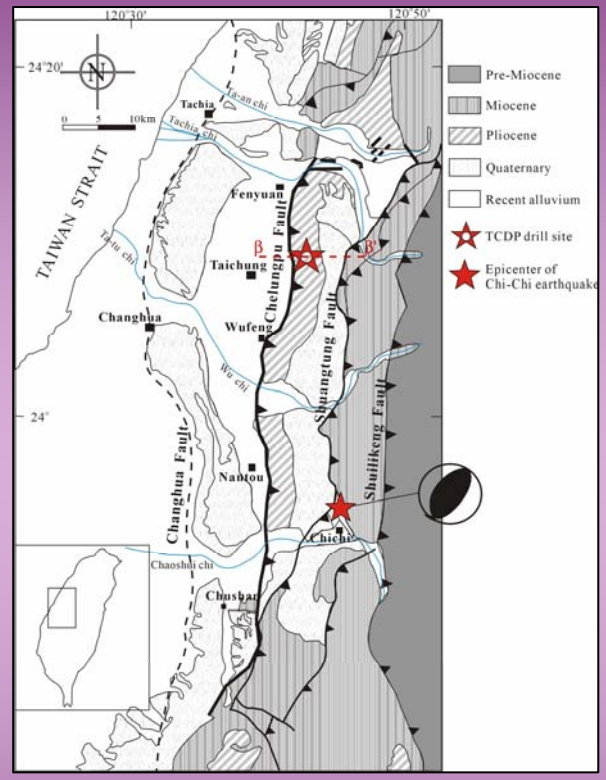

What was the stress state when these cracks were formed ?

Measurements on Hole-B samples

sandstone
siltstone
Fault zones

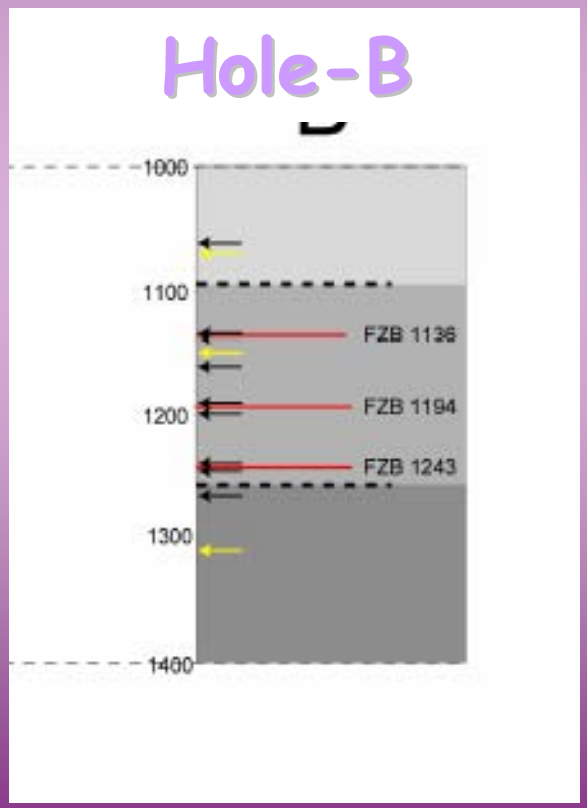

4 sets of three orthogonal samples

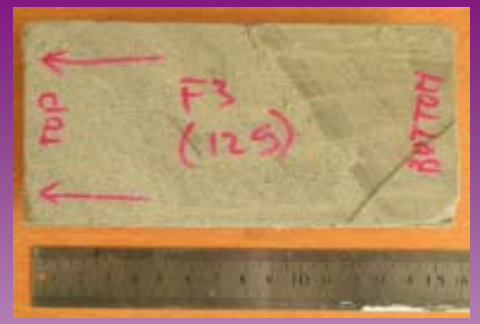

sandstone - formation

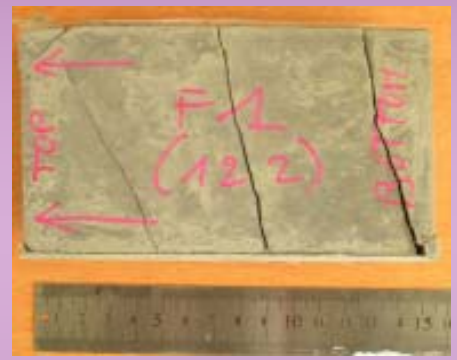

siltstone - formation

21 samples cored
no orthogonal set

siltstone – damaged zones

Hole-B samples: data on AMS

Hole-B

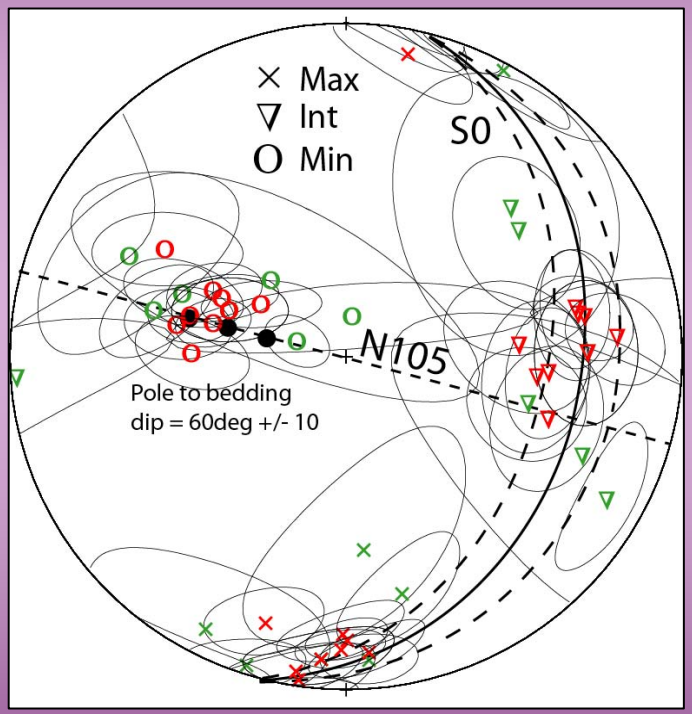

Hole-A

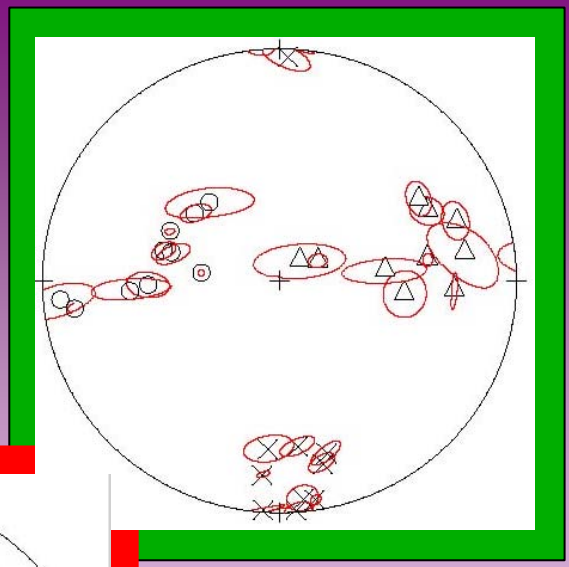

sandstone formation

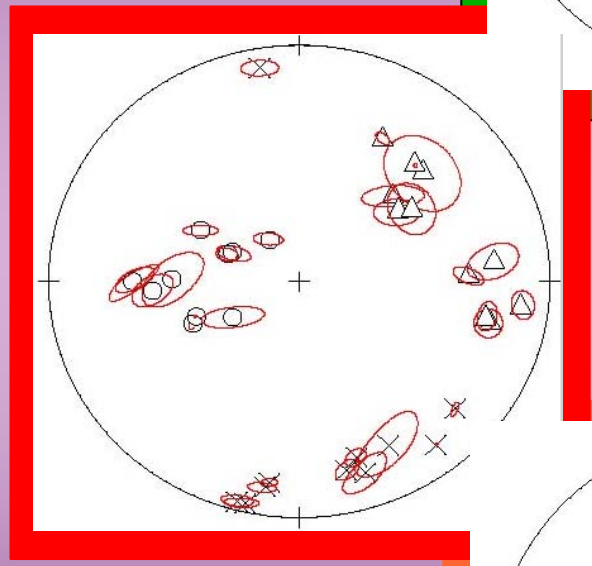

siltstone formation

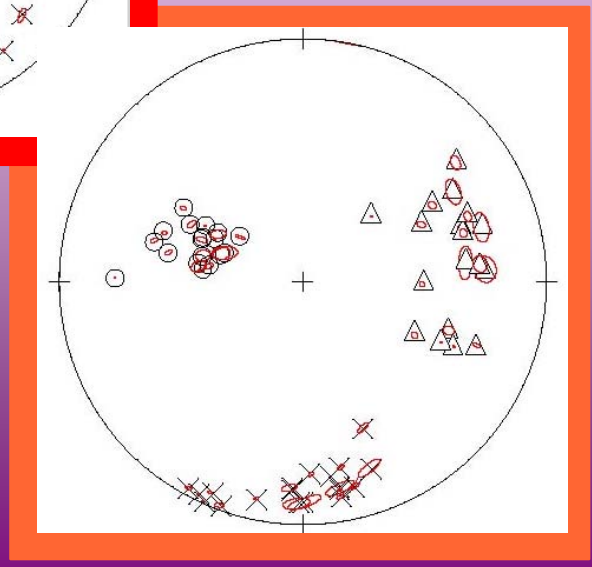

siltstone damaged zones

Hole-B samples: data on AMS

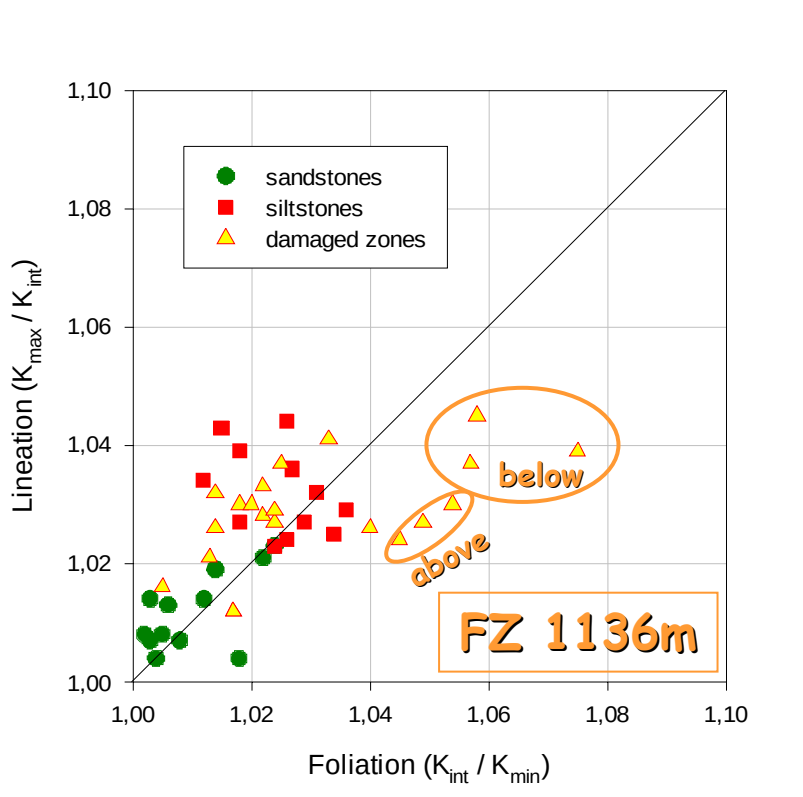

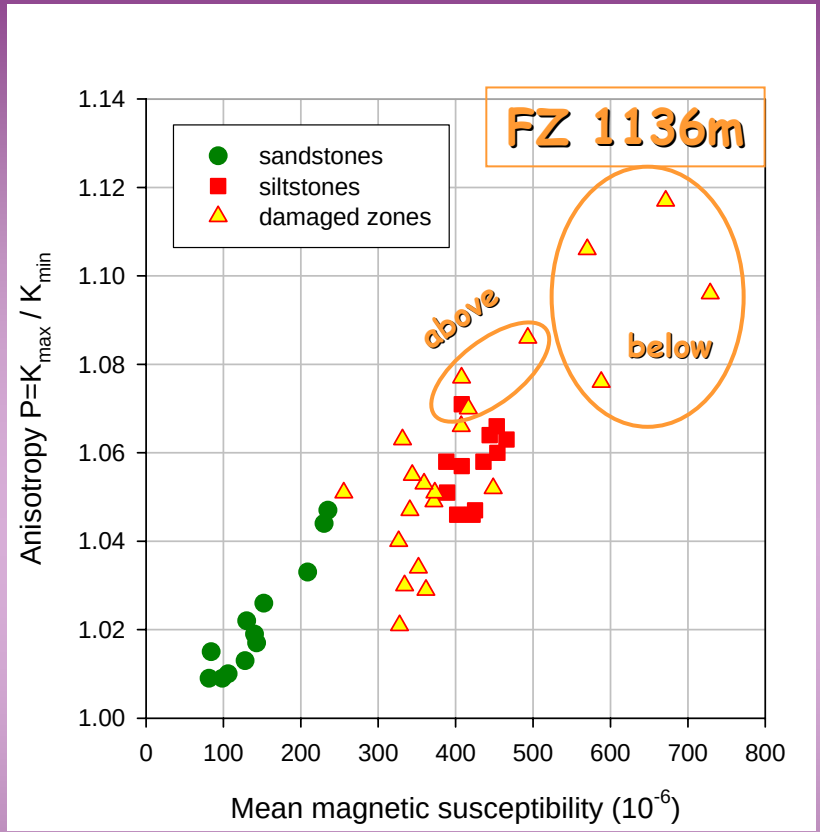

Samples in the damaged zone close to the rupture area of the 1999 earthquake are clearly identified (higher foliation and mean susceptibility)

Hole-B samples: data on elastic anisotropy

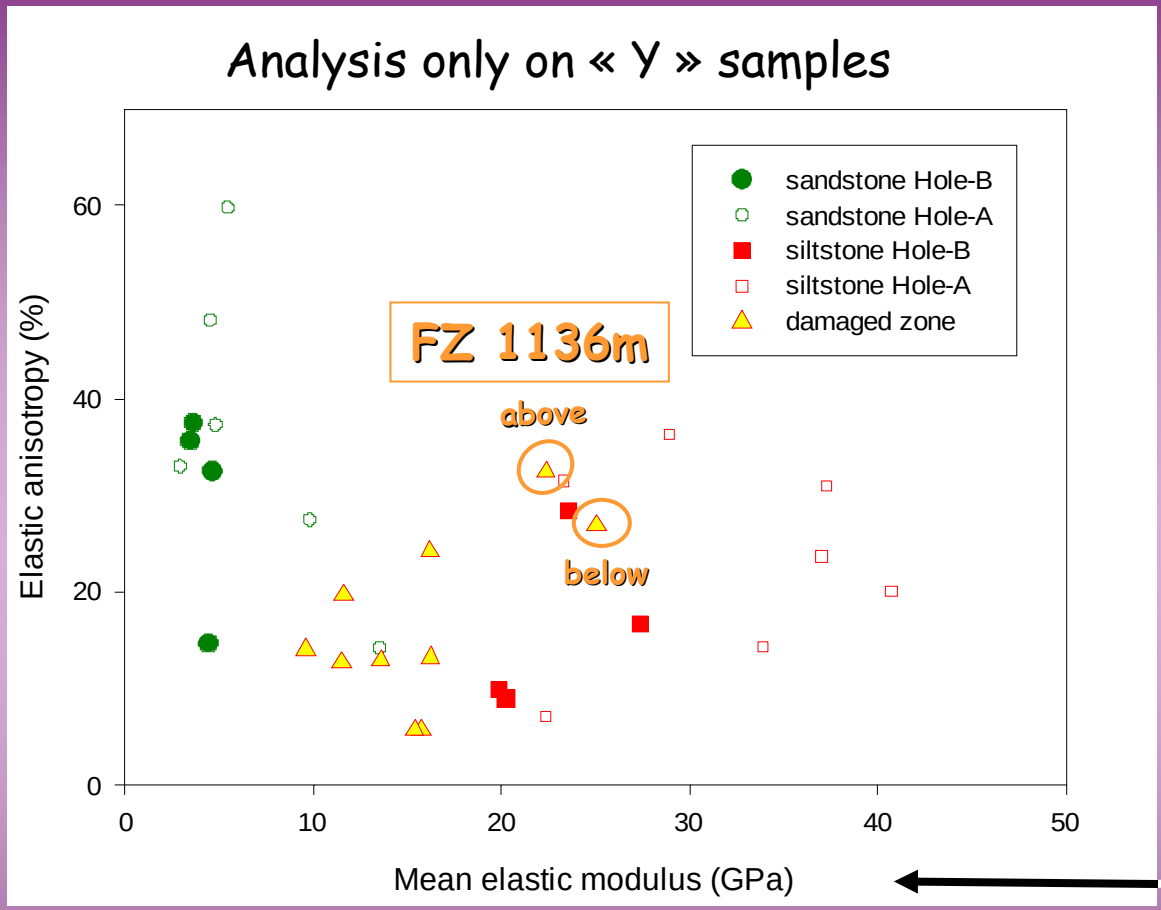

$M = \rho V_p^2$

- Siltstone samples in Hole-B seem to be softer
- Damaged zone samples are intermediate between formation sandstones and siltstones

Evolution of magnetic properties with depth

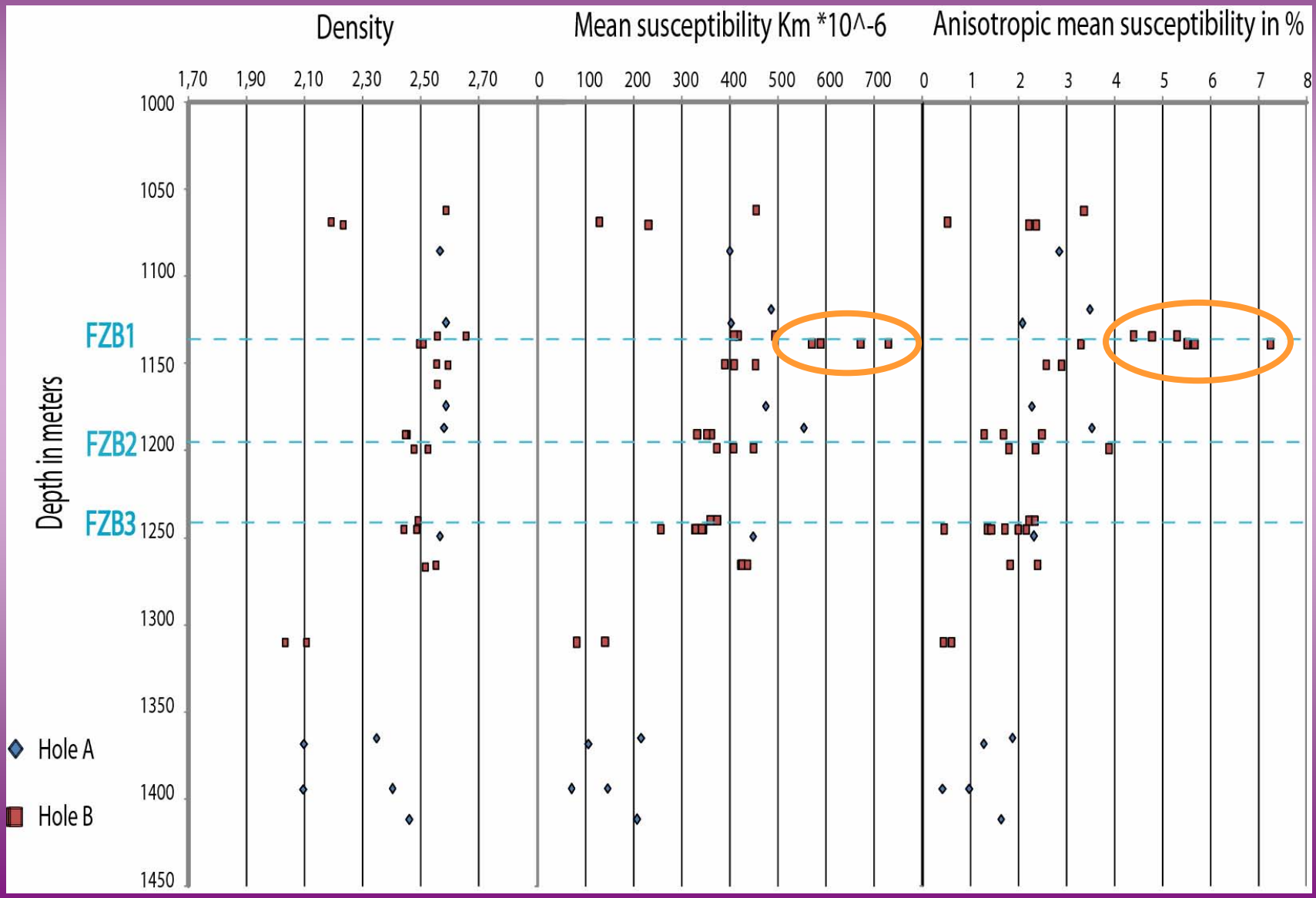

(Hirono et al., GRL 2006)

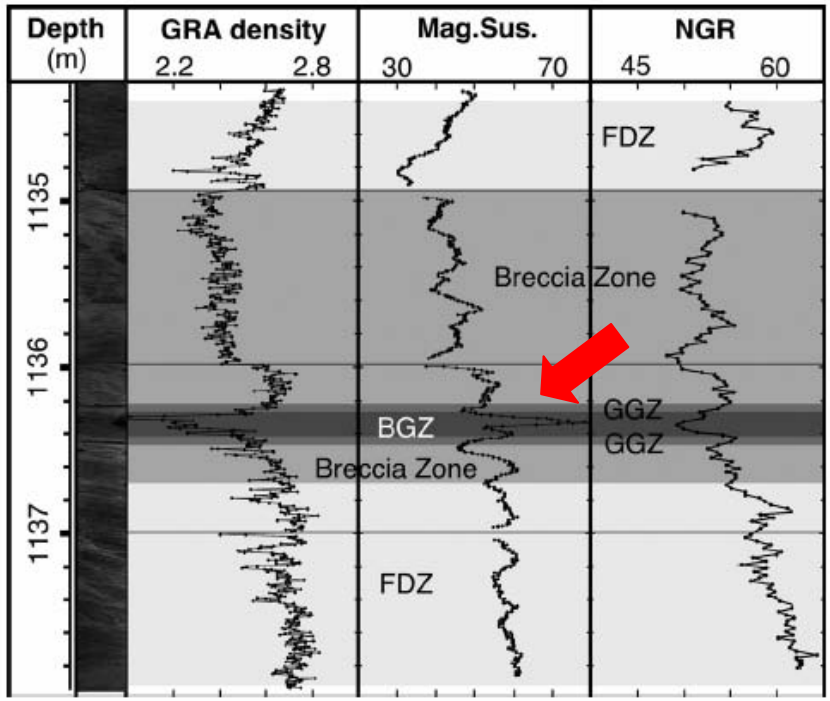

Figure 2. Density, magnetic susceptibility (Mag.Sus.) and natural gamma ray radiation (NGR) logs from 1136mFZ. The units are g/cm^3, 10^{-5}SI, and cps, respectively. FDZ: fracture-damaged zone, BGZ: black gouge zone, GGZ: gray gouge zone.

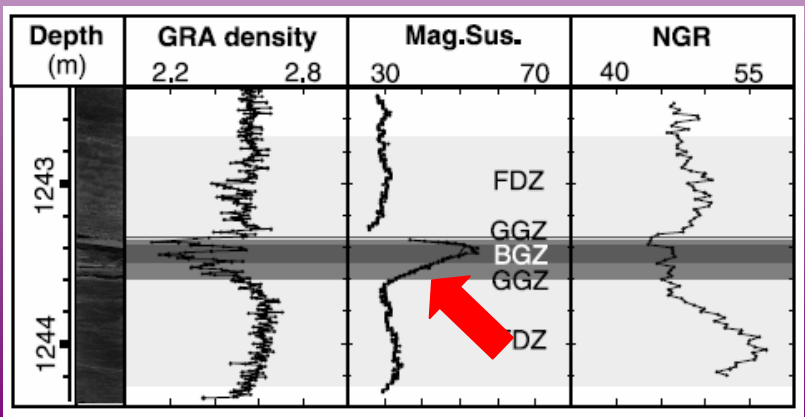

Similar observation by Hirono et al.

mineralogical transformation associated with the slip zones

Observation of microstructures in the fault zones

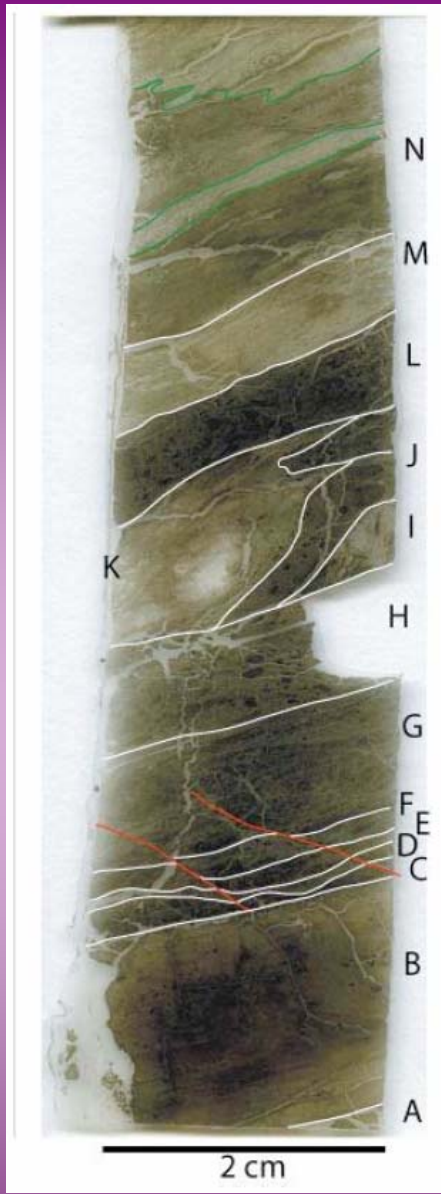

Several zones showing different textures and mineralogical composition

Observation of microstructures in the fault zones

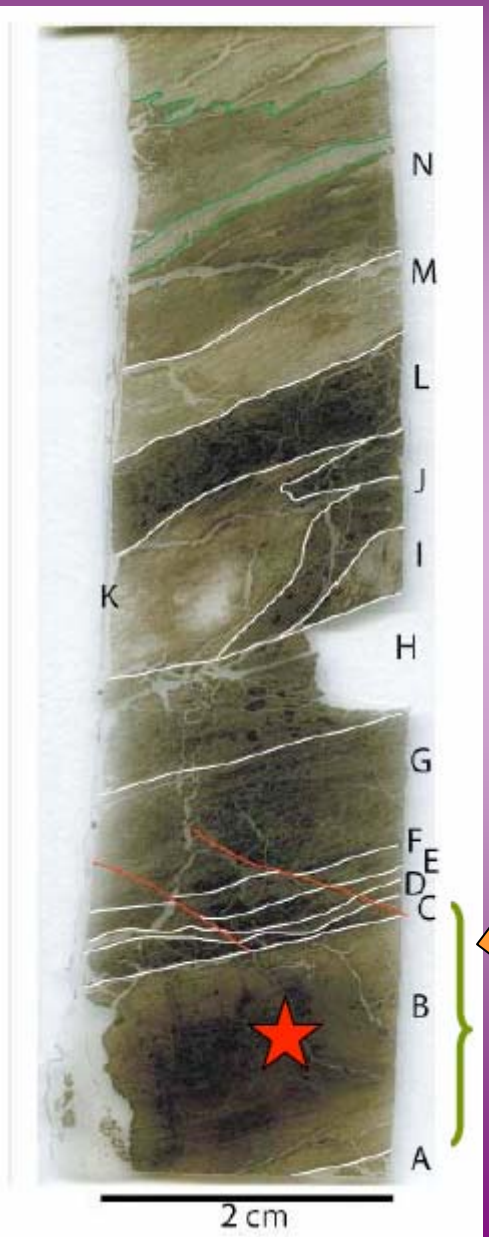

Dark fragments: Pseudotachylytes ?

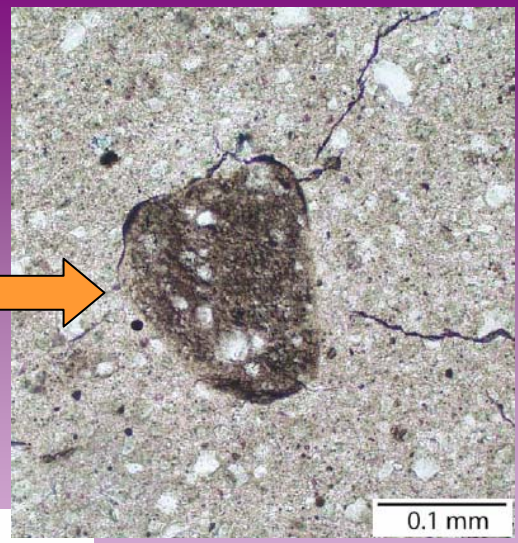

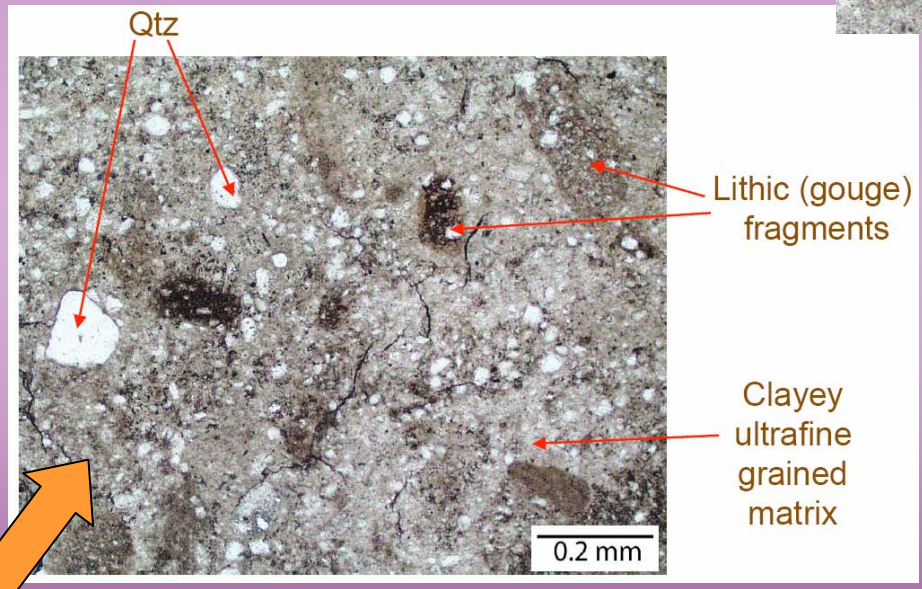

The less deformed layer is B and is interpreted to be the Chi-Chi earthquake slip zone (Ma et al., Nature, 2006)

Main features common to both FZ

- Micas / chlorite apparently absent
- Isotropic zones
- Rolled fragments or clay- clast aggregates (suggests thermal pressurization)
- Preferred orientation of clays
- Calcite veins: hydraulic fracturing (implies fluid redistribution)
- interseismic compaction probably occurs by dissolution-recrystallization

Hole A
FZA 1111 m

Hole B
FZB 1136 m

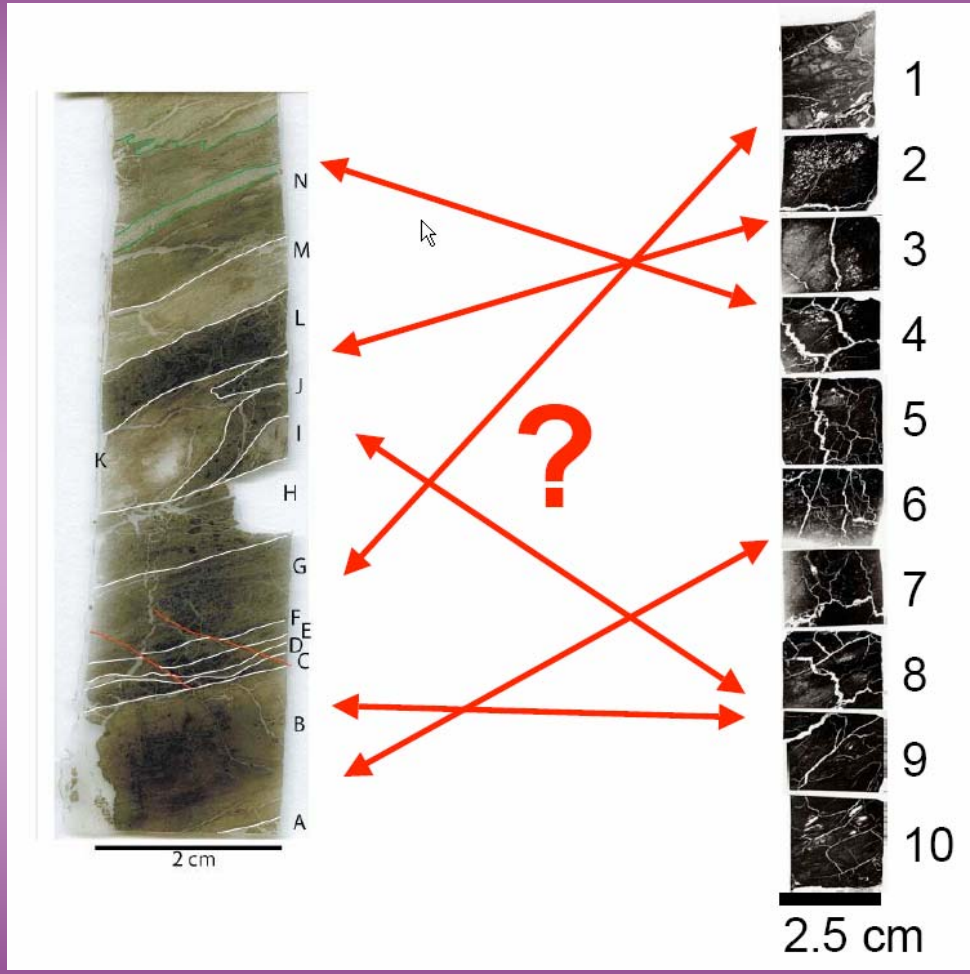

But impossible to exactly correlate the different layers between FZA-1111 and FZB-1136

CONCLUSIONS

1) AMS data are consistent for both sandstones and siltstones, in holes A and B, at all depths, showing that both formations have experienced layer parallel shortening.

2) APV data for sandstones only show the existence of an anisotropic distribution of cracks which orientation is consistent with the local tectonic environment.

3) The analysis of core samples from the damage zones near the identified fault zones in Hole-B shows that there is an anomaly of both AMS and mean susceptibility close to the rupture zone of the 1999 earthquake.

The anisotropic nature of the formations should have a strong influence on fluid transport and hydromechanical behaviour